bioRxiv preprint doi: https://doi.org/10.1101/2021.06.01.446547; this version posted June 2, 2021. The copyright holder for this preprint (which was not certified by peer review) is the author/funder, who has granted bioRxiv a license to display the preprint in perpetuity. It is made available under aCC-BY 4.0 International license.

Catheterized-bladder environment induces hyphal *Candida albicans* formation, promoting fungal colonization and persistence.

Alyssa A. La Bella, Marissa J. Andersen, Alex Molesan, Peter V. Stuckey, Felipe H. Santiago-Tirado*, & Ana L. Flores-Mireles*

Department of Biological Sciences, University of Notre Dame, Notre Dame, IN, USA

*Address correspondence to Ana L. Flores-Mireles (ALFM), afloresm@nd.edu, and Felipe H. Santiago-Tirado(FHST), fsantiago@nd.edu

Mailing address: 351 Galvin Life Science Center, Notre Dame, IN 46556, USA. Phone: (574) 631-4964 (ALFM) and (574) 631-4096 (FHST).

Short title: *Candida*-fibrinogen interactions are critical for CAUTI

Key words: *C. albicans*; CAUTI; UTI; fibrinogen; fibrin; filamentation; hyphae; biofilm; urine; bladder; catheter; candiduria; fungi;

bioRxiv preprint doi: https://doi.org/10.1101/2021.06.01.446547; this version posted June 2, 2021. The copyright holder for this preprint (which was not certified by peer review) is the author/funder, who has granted bioRxiv a license to display the preprint in perpetuity. It is made available under aCC-BY 4.0 International license.

ABSTRACT

Catheter-associated urinary tract infections (CAUTIs) are a serious public health problem and account for approximately 40% of hospital-acquired infections worldwide. *Candida spp* are a major causative agent of CAUTI (17.8%) – specifically *Candida albicans*– that has steadily increased to become the second most common CAUTI uropathogen[1]. Yet, there is poor understanding of the molecular details of how *C. albicans* attaches, grows in the bladder, forms biofilms, survives, and persists during CAUTI [2]. Understanding of the mechanisms that contribute to CAUTI and invasive fungal infection will give insights into the development of more effective therapies, which are needed due to the spread of antifungal resistance and complex management of CAUTI in patients that require a urinary catheter [3]. Here, we characterize the ability of five *Candida albicans* clinical and laboratory strains to colonize the urinary catheter, grow and form biofilm in urine, and their ability to cause CAUTIs using our mouse model. Analysis of *C. albicans* strains revealed that growth in urine promotes morphological transition from yeast to hyphae, which is important for invasive infection. Additionally, we found that biofilm formation was dependent on the presence of fibrinogen, a protein released on the bladder to promote bladder healing[4,5]. Furthermore, deletion of hyphae regulatory genes resulted in defective bladder and catheter colonization and abolished dissemination. These results indicate that novel antifungal therapies preventing the morphological transition of *C. albicans* from yeast to hyphae have considerable promise for the treatment of fungal CAUTIs.

bioRxiv preprint doi: https://doi.org/10.1101/2021.06.01.446547; this version posted June 2, 2021. The copyright holder for this preprint (which was not certified by peer review) is the author/funder, who has granted bioRxiv a license to display the preprint in perpetuity. It is made available under aCC-BY 4.0 International license.

INTRODUCTION

Fungal infections and diseases have become a serious public health concern. *Candida*, *Aspergillus*, and *Cryptococcus spp.* are among the most prominent fungal pathogens contributing to mycoses-related deaths[6,7]. Of these pathogens, *Candida spp.* is the prevailing opportunistic pathogen in addition to being the fourth most common hospital-acquired bloodstream infection (candidemia) in the United States[6,8]. More specifically, *Candida albicans* is the main contributor to invasive candidiasis, responsible for 50% to 70% of candidiasis cases[6,8]. As *Candida spp.* are becoming increasingly resistant to antifungal therapy[9], the management of this fungal pathogen is a major challenge for the medical community[8].

C. albicans inhabits the gastrointestinal and genitourinary tracts and mucosal membranes along with forming biofilms on dentures, pacemakers, prosthetic joints, and intravenous and urinary catheters[10-12]. The 2016 National Healthcare Safety Network (NHSN) review found that *Candida spp.,* specifically *Candida albicans,* have become the second most prevalent uropathogen causing 17.8% of catheter associated urinary tract infections (CAUTIs)[1]. CAUTIs are the most common hospital-acquired infection (HAI) with more than 150 million individuals acquiring such an infection each year[13,14]. The use of catheters and subsequent infections are not limited to hospital-care settings. In long-term care facilities such as skilled nursing facilities (SNF), 12.6% of admitted patients use an indwelling catheter. Further, in nursing homes, 11.9% of residents use indwelling catheters[15], and ~50% of nursing home residents with indwelling urinary catheters will experience symptomatic CAUTIs[16]. Despite *Candida spp*. prevalence in CAUTIs, we lack a clear understanding of the factors required for *Candida* pathogenesis during CAUTIs [1,2].

C. albicans, among other fungal species, can grow in yeast, pseudohyphal, and hyphal morphologies[17-19]. The pseudohyphal and hyphal form have a filamentous structure with the

bioRxiv preprint doi: https://doi.org/10.1101/2021.06.01.446547; this version posted June 2, 2021. The copyright holder for this preprint (which was not certified by peer review) is the author/funder, who has granted bioRxiv a license to display the preprint in perpetuity. It is made available under aCC-BY 4.0 International license.

pseudohyphae containing constrictions at sites of septation and hyphae having long tube-like filaments with no constrictions at the site of septation. *C. albicans*' ability to undergo morphological changes is a virulence determinant. The hyphae morphology is critical in the spread of infection and results in *Candida* becoming virulent. When *C. albicans* is in its hyphae morphology, it can invade epithelial and endothelial cells, resulting in tissue damage and an invasive infection. *C. albicans* can be converted to its hyphae form via serum, neutral pH, and other environmental conditions such as CO_2, and is controlled by the master regulator Enhanced filamentous growth protein 1 (Efg1), among other transcription factors[20].

The switch between yeast and hyphal forms is essential to pathogenesis and biofilm formation[10,19-22]. Most *C. albicans* infections are associated with biofilm formation, making biofilm formation one of the main virulence traits of candidiasis. The biofilm initiates with the adherence of yeast cells to a surface, forming microcolonies followed by proliferation of hyphae and pseudohyphae[21]. Maturation of the biofilm occurs when the hyphal scaffold is encased in an extracellular polysaccharide matrix, other carbohydrates, proteins, nucleic acids and lipids[23,24]. The final step in biofilm formation involves dispersion of non-adherent yeast cells for establishment of colonization and biofilms into the surrounding environment[21]. The resulting biofilm poses a serious threat to the host as the biofilm cells grow increasingly resistant to antifungal therapy and can evade protection from the host defenses[24]. New antifungal treatments, such as the echinocandins, that target the β-1,3 glucan component of the cell wall have proven to successfully prevent *C. albicans* biofilms[11,25]; unfortunately, recently echinocandin-resistant *Candida spp* are emerging[26,27].

Candiduria (*Candida* in urine) is primarily associated with patients with predisposing factors including diabetes mellitus, genitourinary structural abnormalities, diminished renal

bioRxiv preprint doi: https://doi.org/10.1101/2021.06.01.446547; this version posted June 2, 2021. The copyright holder for this preprint (which was not certified by peer review) is the author/funder, who has granted bioRxiv a license to display the preprint in perpetuity. It is made available under aCC-BY 4.0 International license.

function, renal transplantations, metabolic abnormalities, and indwelling urinary tract catheters or devices[28]. *C. albicans* colonization and overgrowth in different infection models have been associated with dysbiosis in the host environment such as alterations in host immunity, stress, and resident microbiota[10]. Importantly, urinary catheterization disrupts the bladder homeostasis, mechanically compromising the integrity of the urothelium, inducing inflammation, interfering with normal micturition (voiding)[29], and disrupting host defenses in the bladder[30-32]. Hence, we are interested in understanding how these host environment changes, specifically in the bladder, can promote fungal CAUTI.

The inflammation response caused by catheterization exposes cryptic epithelial receptors or recruits host factors that can be recognized by the pathogen, enabling microbial colonization, multiplication, and persistence within the urinary tract[30-33]. We have found that one of these factors is fibrinogen (Fg), which is released into the bladder to heal damage tissue and prevent bleeding due to catheter-induced inflammation in both mice and humans[5,34,35]. However, due to the constant mechanical damage caused by the urinary catheter, Fg accumulates in the bladder and deposits onto the catheter at concentrations that increase with prolonged catheterization[5,34,36-38]. This Fg is used by *Enterococcus faecalis* and *Staphylococcus aureus* for colonization of catheters and the bladder through the adhesins Ebp and ClfB, respectively; blocking this interaction resulted in defective to no colonization[34,36,39]. Similarly, we have found that in *Acinetobacter baumannii* and *Proteus mirabilis* CAUTI, interactions with Fg are important[40,41]; however, the bacterial factors responsible have not yet been described. Consistently, in an *ex vivo* study we showed that a *C. albicans* CAUTI isolate binds to urinary catheters via Fg[5]. This strongly suggests that urine is inducing changes in the expressed Fg-binding adhesins, prompting us to study this interaction more carefully in *C. albicans*.

bioRxiv preprint doi: https://doi.org/10.1101/2021.06.01.446547; this version posted June 2, 2021. The copyright holder for this preprint (which was not certified by peer review) is the author/funder, who has granted bioRxiv a license to display the preprint in perpetuity. It is made available under aCC-BY 4.0 International license.

In this study, we characterized five *C. albicans* clinical and laboratory strains' growth in urine, biofilm formation, and capability to cause CAUTI. We found that for the *C. albicans* strains that grew poorly in urine, growth was promoted when supplemented with a nitrogen source. Urine itself promoted morphological changes, and biofilm formation was enhanced by the presence of protein and Fg in urine conditions. Furthermore, *C. albicans* was able to infect the catheterized bladder and form a biofilm on the urinary catheter; importantly, a hyphae-deficient mutant was unable to cause CAUTI, suggesting that filamentation was critical for this infection model. Based on these findings, we conclude that the morphological change of *C. albicans,* which is promoted by urine and the catheterized environment, is crucial to colonize, persist, and cause CAUTIs.

RESULTS

C. albicans survives and grows in urine.

C. albicans is able to infect a wide range of human sites including oropharyngeal, gastrointestinal, intra-abdominal, skin, genital, and urinary tract, demonstrating its plasticity to survive and replicate in different host environments[42,10,11,13,14,20]. Since *C. albicans* has become a prominent CAUTI pathogen, we explored its ability to grow in urine using clinical and laboratory strains. We used three urinary clinical isolates Pt62, Pt65, and PCNL1[5,43] (obtained from Washington University School of Medicine) and two well-characterized laboratory strains, DAY230 and SC5314 (**Table S3**). Since hyphal formation is important for promoting disease, we used a hyphae defective mutant in the SC5314 background, *efg-1*Δ*cph-1*Δ, to test whether hyphal formation is important in the catheterized bladder environment (**Table S3**). We tested their ability to grow in a variety of environments ranging from nutrient rich to restrictive conditions. For rich environment, we used yeast extract peptone dextrose (YPD) and brain and heart infusion (BHI) in shaking and

bioRxiv preprint doi: https://doi.org/10.1101/2021.06.01.446547; this version posted June 2, 2021. The copyright holder for this preprint (which was not certified by peer review) is the author/funder, who has granted bioRxiv a license to display the preprint in perpetuity. It is made available under aCC-BY 4.0 International license.

static conditions; YPD is a standard *C. albicans* growth media and BHI was used since the clinical strains were isolated on this media. Static growth was used to mimic the bladder environment and shaking growth was used as a comparison with standard lab culture conditions. For restrictive environment, we used human urine and to further mimic the plasma protein extravasation in the catheterized bladder[37], urine was supplemented with either 3% human serum or different nitrogen sources including amino acids (AA), bovine serum albumin (BSA), or Fg. Serum albumin and Fg are two of the most abundant host proteins on catheters retrieved from human and mice and have shown to be used by other uropathogens as a nutrient source[34,36]. Samples were taken at 0 hours, 24 hours, and 48 hours to assess growth by enumeration of colony forming units (CFUs). As expected, *C. albicans* clinical and laboratory strains grow in higher densities in rich media and aeration while growth in rich media in static conditions was similar to the urine conditions (**Fig. 1**). In restrictive environment, *C. albicans* strains were able to survive and replicate in urine, but it varied widely between the strains and supplementation. Human serum supplementation promoted growth of all strains by 24 hrs with a subsequent decline, possibly because all nutrients were consumed (**Fig. 1**). The growth of the lab strains and Pt62 was not enhanced, or was inhibited, with BSA or Aa supplementation when compared with urine alone (**Fig. 1A, D-F**). However, Fg enhanced growth of all strains, at different magnitudes when compared with urine alone (**Fig. 1**), except for PNCL1, which already exhibited good growth in urine alone (**Fig. 1C**).

Urine conditions promotes *C. albicans* hyphal formation.

Environmental conditions induce *C. albicans* morphological changes that are associated with virulence[10,19]. *C. albicans* can exhibit different morphologies[21], but the main ones are vegetative yeast, pseudohyphae, and hyphae[19]. Hyphae morphology leads to the spread of infection and

bioRxiv preprint doi: https://doi.org/10.1101/2021.06.01.446547; this version posted June 2, 2021. The copyright holder for this preprint (which was not certified by peer review) is the author/funder, who has granted bioRxiv a license to display the preprint in perpetuity. It is made available under aCC-BY 4.0 International license.

increased virulence of the pathogen[20,22]. Therefore, we wanted to determine how the bladder environment affects *C. albicans* morphology. To assess the pathogen morphologies, *C. albicans'* laboratory and clinical strains were grown in urine with 3% human serum to mimic plasma protein extravasation in the catheterized bladder[37,38]. YPD alone was used as a negative control and when supplemented with serum was used as a positive control for inducing hyphal morphology[44-46]. Strains were incubated at 37ºC with 5% CO_2 for 48 hrs and samples were collected at 0, 24, and 48 hours. *C. albicans* strains were stained with calcofluor white to assess morphology using fluorescence microscopy (Zeiss Axio Observed inverted scope). The cell morphology was analyzed automatically using CellProfiler software (available from the Broad Institute at www.cellprofiler.org)[47] to quantify the percentages of yeast, pseudophyphal, or hyphal forms based on the circularity value of each outlined cell (**Fig. 2G, Table S1**). All strains showed predominantly yeast morphology in YPD media and YPD with serum induced pseudohyphal and hyphal formation in all strains, except Pt65 and SC5314 *efg-1*Δ*cph-1*Δ. Notably, our analysis showed that urine conditions promote pseudohyphal and hyphal formation in all strains (**Fig. 2, Table S1**) except SC5314 *efg-1*Δ*cph-1*Δ (**Fig. 2F, Table S1**). Pseudohyphal and hyphal morphologies were further induced when urine was supplemented with human serum in Pt62, PNCL1, DAY230, and SC45314 but not in Pt65. This suggests that the catheterized environment triggers *C. albicans* morphological change from the yeast cell form to hyphae.

Fibrinogen enhances *C. albicans'* biofilm formation.

Scanning electron microscopy analyses of *C. albicans* biofilms on urinary catheters from CAUTI patients[2,43] and rats[48,49] have revealed pseudohyphal and hyphal morphology. During candidiasis, *C. albicans* pseudohyphal and hyphal formation induces expression of virulence genes including

bioRxiv preprint doi: https://doi.org/10.1101/2021.06.01.446547; this version posted June 2, 2021. The copyright holder for this preprint (which was not certified by peer review) is the author/funder, who has granted bioRxiv a license to display the preprint in perpetuity. It is made available under aCC-BY 4.0 International license.

188 host adhesion factors[18,21,50,51]. One of those factors is Mp58, a Fg-binding protein[4,52]. In an *ex-vivo*
189 study, we showed that *C. albicans* PNCL1 clinical isolate colocalized with Fg-deposited on urinary
190 catheters retrieved from a patient with preoperative negative urine culture[5]. Fg deposition has been
191 shown to be a platform for biofilm formation by diverse uropathogens[5,34,36,41,53], suggesting that
192 Fg may be an important factor to promote *C. albicans* CAUTI pathogenesis. Based on these and
193 our previous findings (**Fig. 2**), we hypothesized that urine conditions induce factors responsible
194 for Fg-binding and biofilm formation. Thus, we assessed biofilm formation under rich (YPD and
195 BHI) and restrictive conditions (human urine) and compared between BSA- and Fg-coated
196 microplates as we have previously described[54]. At 48 hrs, immunostaining analyses were
197 performed to assess fungal biofilm formation by using anti-*Candida* antibodies and biofilm
198 biomass was quantified by fluorescence intensity[54]. We found that for the clinical strains, Fg
199 promoted biofilm formation in all conditions but Fg-dependent biofilm formation was further
200 enhanced in human urine condition (**Fig. 3A-C**). For the laboratory strains, we found a similar
201 Fg-dependent biofilm formation in YPD, BHI, and urine, but Fg had no effect in DAY230 when
202 grown in BHI (**Fig. 3D and E**). In contrast, SC5314 *efg-1*Δ*cph-1*Δ was not able to form biofilms
203 in human urine regardless of the coated surface (**Fig. 3F**), highlighting the importance of
204 filamentation for biofilms under urine conditions. Notably, we observed that the hyphae-defective
205 mutant was able to form Fg-dependent biofilms in YPD and BHI (**Fig. 3F**), suggesting that the
206 mechanisms of biofilm formation are different. This difference could be related to adhesins that
207 are expressed during yeast form that may contribute to biofilm but not in urine conditions.
208 Therefore, using conditions that closely mimic the *in vivo* environment are important to identify
209 physiologically-relevant determinants for biofilm formation.
210

bioRxiv preprint doi: https://doi.org/10.1101/2021.06.01.446547; this version posted June 2, 2021. The copyright holder for this preprint (which was not certified by peer review) is the author/funder, who has granted bioRxiv a license to display the preprint in perpetuity. It is made available under aCC-BY 4.0 International license.

Fibrinogen promotes *C. albicans* biofilm formation.

Furthermore, we analyzed the *C. albicans* strains biofilm by immunofluorescence (IF) microscopy. *C. albicans* strains' biofilms were grown for 48 hrs in human urine using glass-bottom petri dishes coated with BSA or Fg. Biofilms on BSA were barely monolayers or small aggregates composed of yeast, pseudohyphae, and hyphae (**Fig. 3G-K**), except for SC5314 *efg-1*Δ*cph-1*Δ, where all cells were in yeast form (**Fig. 3L**). On the other hand, Fg promoted a robust biofilm in all strains when compared with BSA-dependent biofilms (**Fig. 3G-K**); except for the hyphae-deficient mutant where the colonization was composed of small yeast aggregates similar to the colonization on BSA-coated surfaces (**Fig. 3L**), suggesting filamentation is important for Fg-dependent biofilm formation.

Furthermore, in the damaged tissue environment, like the catheterized bladder, Fg is converted into fibrin fibers or nets to stop bleeding and allow healing. Therefore, we explored the fungal-fibrin interactions *in vitro*. Fibrin fibers and nets were formed in glass-bottom petri dishes by adding thrombin to soluble Fg and incubating at 37°C for an hour; then, *C. albicans* strains were added and incubated for 48 hrs at 37°C in human urine. Visualization of the interaction was done by confocal microscopy and 3D reconstruction at 10x and 40x. We found that most of the cells had a pseudohyphal and hyphal morphology surrounding and going through the fibrin fibers and nets (**Fig. 4A-E**), except for SC5314 *efg-1*Δ*cph-1*Δ (**Fig. 3F**).

C. albicans hyphal formation is critical for establishment of CAUTI.

Based on our previous results, we hypothesized that a hyphae-deficient mutant of *C. albicans* would have a defective colonization in the catheterized bladder. To test this, we assessed the ability of the clinical and laboratory strains to colonize and form biofilm on the urinary catheter using our

bioRxiv preprint doi: https://doi.org/10.1101/2021.06.01.446547; this version posted June 2, 2021. The copyright holder for this preprint (which was not certified by peer review) is the author/funder, who has granted bioRxiv a license to display the preprint in perpetuity. It is made available under aCC-BY 4.0 International license.

established CAUTI mouse model[34,36-41,55-57]. Furthermore, to get a better understanding of the contribution of the catheterized bladder environment to *C. albicans'* colonization, we carried out infections in catheterized and non-catheterized mice. Mice with or without catheters were challenged with 1×10^6 CFU of each strain grown in YPD media overnight at 37°C under static conditions. After 24 hours post infection (hpi), the mice were euthanized and their organs and catheters (when catheterized) were harvested to quantify colonization by CFU enumeration. The results showed that catheterization significantly increased colonization on the bladder of Pt62, Pt65, PNCL1, DAY230 and SC5314 and the catheter and bladder were colonized to the same extent (**Fig. 5**). Importantly, we found that the hyphae-deficient mutant, SC5314 *efg-1*Δ*cph-1*Δ, had a significantly defective bladder and catheter colonization when compared with the SC5314 wild-type (WT) strain (p-value < 0.005; **Fig. 5E**). Interestingly, in the absence of a catheter, the hyphae-deficient mutant behaved and colonized to the same extent as the WT strain.

In human infection, the incidence of candidemia and systemic dissemination arising from *Candida* UTI or candiduria *Candida* in urine are relatively low (1-8% of all candidemia cases)[58]. However, the prevalence of candidemia due to candiduria increases in critically ill and immunocompromised patients[59,60], especially if the patients are undergoing urinary catheterization[61]. Since our mouse model of CAUTI allows us to assess dissemination, we analyzed fungal burden of kidneys, spleen, and heart after 24 hpi (**Fig. 5**). We found that urinary catheterization significantly contributes to the fungal spread of DAY230 to the kidneys and spleens (p-value < 0.05; **Fig. 5D**) and in SC5314, spreads to the kidneys (p-value < 0.005; **Fig. 5E**). Additionally, colonization of the kidneys by Pt62 and Pt65 was 2-3 logs higher than non-catheterized mice, trending to significance. Furthermore, the hyphae-deficient mutant, SC5314 *efg-1*Δ*cph-1*Δ, did not show differential dissemination between catheterized and non-catheterized

bioRxiv preprint doi: https://doi.org/10.1101/2021.06.01.446547; this version posted June 2, 2021. The copyright holder for this preprint (which was not certified by peer review) is the author/funder, who has granted bioRxiv a license to display the preprint in perpetuity. It is made available under aCC-BY 4.0 International license.

mice (**Fig. 5E**). This data showed that the changes induced by the presence of a catheter are necessary for fungal colonization of the urinary tract and further demonstrate that hyphal morphology as well as pathways regulated by *efg-1* and *cph-1* are crucial for establishment of CAUTI.

Interactions with fibrinogen and hyphal morphology are important for *C. albicans* colonization the catheterized bladder.

To further understand the *C. albicans'* morphology, its interaction with Fg, and its spatial colonization in the bladder during CAUTI, we performed histological analyses using hematoxylin and eosin (H&E) staining, and also IF microscopy of 24 hpi implanted and infected bladders with 1 x 10^6 CFU of each *C. albicans* strain. For the IF analysis, we stained for *C. albicans* (red), Fg (green), and for neutrophils (white) (**Fig. 6,** merge images; **Fig. S1-S6**, single channels). We focused on neutrophils for two reasons: we have shown they are highly recruited into the catheterized bladder[37,38,62] and the fact that neutropenic patients are more susceptible to *C. albicans* and bacterial dissemination from CAUTI[59,63-65], suggesting a role in controlling candidemia from candiduria. We found that bladder colonization was so robust that it was visible in the H&E-stained whole bladders (blue arrow heads) (**Fig. 6**). Consistently, our IF analysis showed the presence of *C. albicans'* hyphal and pseudohyphal morphologies in the lumen of the bladder in all clinical and laboratory strains (**Fig 6A-D**), except for the hyphal mutant, SC5314 *efg-1*Δ*cph-1*Δ (**Fig. 6F**). As seen with other uropathogens, including *E. faecalis*, *S. aureus*, *A. baumannii*, and *P. mirabilis*[5,34,36,40,41,53], *C. albicans* cells in the catheterized bladder are found in close association with Fg (**Fig. 6** and **Fig. S1-S6**).

bioRxiv preprint doi: https://doi.org/10.1101/2021.06.01.446547; this version posted June 2, 2021. The copyright holder for this preprint (which was not certified by peer review) is the author/funder, who has granted bioRxiv a license to display the preprint in perpetuity. It is made available under aCC-BY 4.0 International license.

Importantly, neutrophils were highly recruited into the bladder, specifically in the areas with fungal colonization (**Fig. 6** and **Fig. S1-S6**). We found that *C. albicans* breached the urothelium, encountering a strong neutrophil response at the site of entry (**Fig. 6C-E** and **Fig. S3-S4**). For example, we found that PNCL1 was able to reach the bladder lamina propria, inducing a massive neutrophil recruitment to contain the infection (**Fig. 6C** and **Fig. S3**). Pt62 and Pt65 cells were primarily found on the bladder lumen and the fungal cells were interacting with Fg and neutrophils (**Fig. 6A-B** and **Fig. S3-S4**). On the other hand, robust fungal colonization and neutrophil recruitment was not observed in the SC5314 *efg-1*Δ*cph-1*Δ infected bladder (**Fig. 6F** and **Fig. S6**). These data demonstrate that in the catheterized bladder, *C. albicans* is mostly in hyphal and pseudohyphal morphology and it is able to interact with Fg. Furthermore, neutrophils are recruited to control fungal infection.

C. albicans interacts with deposited fibrinogen on the catheter during CAUTI.

Based on our *in vitro* Fg-binding results, we assessed if *C. albicans*-Fg interaction occurs *in vivo* on the catheter during CAUTI. Catheters from mice infected with each strain were retrieved 24 hpi and immunostained for *C. albicans* (red) and Fg (green). Except for the hyphal mutant, we found that all strains form a robust biofilm on the implanted catheter (**Fig. 7**), colonizing 59% to 79% of the surface of the catheter (**Table S2**). SC5314 WT showed 78.9 ± 14% colonization of the catheters while SC5314 *efg-1*Δ*cph-1*Δ catheters' colonization was 10.4 ± 7.5%, exhibiting a significant defective colonization (**Fig. 7F-G, L; Table S2**). Our IF analysis showed that *C. albicans* strains were preferentially binding onto deposited Fg on the catheter (**Fig. 7B-G**). We then further quantified the percentage of the catheter-colonizing fungal population that was colocalizing with Fg. We found that 75% to 91% of the *C. albicans* strains' staining was

bioRxiv preprint doi: https://doi.org/10.1101/2021.06.01.446547; this version posted June 2, 2021. The copyright holder for this preprint (which was not certified by peer review) is the author/funder, who has granted bioRxiv a license to display the preprint in perpetuity. It is made available under aCC-BY 4.0 International license.

colocalized with deposited Fg (**Fig. 7H-L**). Moreover, in the SC5314 *efg-1*Δ*cph-1*Δ strain, that was only able to colonize 10% of the catheter (**Fig. 7G, Table S2**), 79% of it was colocalizing with Fg (**Fig. 7L**). This result further corroborates that hyphal formation is important for a robust biofilm formation during CAUTI and that Fg serves as a platform for catheter colonization *in vivo*.

DISCUSSION

In this study, we have shown that hyphal morphology and fungal interactions with Fg and fibrin are critical for establishment of CAUTI. We showed that *C. albicans* is able to survive and grow in urine and supplementation with 3% serum and Fg promotes growth. Importantly, we found that hyphal formation is induced by urine conditions *in vitro* and *C. albicans* strains exhibit pseudohyphal and hyphal morphology *in vivo* during CAUTI. The presence of Fg and fibrin enhances biofilm formation *in vitro* and *in vivo*. Thus, the catheterized bladder (consisting of urine with serum protein and high Fg and fibrin) creates the ideal environment for *C. albicans* to colonize and persist in the host.

Our results showed that hyphal formation was critical for Fg-dependent biofilm formation in urine conditions but not in YPD and BHI media. This seemingly contradictory result is not surprising since we have observed that laboratory growth media do not fully recapitulate conditions found within the host. For example, several factors critical for bacterial biofilm formation in CAUTI are dispensable in *in vitro* biofilm assays when using conventional laboratory growth media[34,38,54-56,66]. Moreover, host proteins have been shown to contribute to fungal biofilm formation[49,67]. A study done by the Andes group found Fg, as well as other host proteins associated with *C. albicans* biofilms in urinary catheters. retrieved from rats[24]. These results, taken together

bioRxiv preprint doi: https://doi.org/10.1101/2021.06.01.446547; this version posted June 2, 2021. The copyright holder for this preprint (which was not certified by peer review) is the author/funder, who has granted bioRxiv a license to display the preprint in perpetuity. It is made available under aCC-BY 4.0 International license.

with our previous data showing that Fg is accumulated in the bladder and deposited on the catheters [1,5,13], and that Fg promotes fungal biofilm formation in urine conditions and during urinary catheterization (**Fig. 3, 5-6**), suggest that expression of Fg binding proteins could mediate fungal biofilm formation in CAUTI.

It has been reported that *C. albicans* encodes a Fg-binding protein, Mp58, which is expressed during candidiasis[4,52]. Furthermore, other cell surface adhesins such as Agglutinin-like sequence (ALS) glycoproteins, hyphal regulated gene 1 (Hyr1), and hyphal wall protein 1 (Hwp1) have shown to be important in biofilm formation[68-72]. From these adhesins, ALS1, ALS3, and ALS9 have been shown to bind to Fg *in vitro*[72-74] and structural analyses have shown binding to Fg γ-chain via protein-protein interaction, similar to Clf adhesins in *S. aureus*[74,75]. However, the role of Mp58, ALSs, Hyr1, and Hwp1 on binding to Fg and their contribution to catheter and bladder colonization during CAUTI have not been described. These adhesins will be explored in further studies.

Interestingly, Mp58, ALSs, Hyr1, and Hwp1 are specifically expressed during hyphal formation[4,52,76-79]. Transition between yeast and hyphae is central to virulence and this shift is responsive to the environment[10,19,20,22,79]. Our results have shown that urine conditions and the catheterized bladder environment induce hyphal formation, which suggest these adhesins and other virulence factors may be expressed during CAUTI. Importantly, we have shown that SC5314 *efg*-1Δ*cph*-1Δ hyphal mutant exhibited defective biofilm formation and Fg binding in urine condition. Furthermore, it displayed deficient catheter and bladder colonization during urinary catheterization. Therefore, Efg1 and Cph1 downstream targets such as Hwp1, Hwp2, Hyr1, ALS8, and secreted aspartyl proteinases (SAP)-4, -5, -6, and -9[80,81] may play independent roles in *C. albicans* CAUTI pathogenesis. Since the Efg1 and Cph1 regulatory networks are known,

bioRxiv preprint doi: https://doi.org/10.1101/2021.06.01.446547; this version posted June 2, 2021. The copyright holder for this preprint (which was not certified by peer review) is the author/funder, who has granted bioRxiv a license to display the preprint in perpetuity. It is made available under aCC-BY 4.0 International license.

348 dissection of their contributions to fungal infection in the catheterized bladder will be further
349 explored.

350 Hyphal cells are important for the formation of biofilms and tissue invasion[70,82-84]. This
351 correlates with our observation that strains were in primarily hyphal morphology on the biofilms
352 and we observed hyphal invasion of urothelium and lamina propria during CAUTI. Importantly,
353 massive neutrophil recruitment occurred into the areas of fungal tissue invasion; this was not
354 observed in the SC5314 *efg*-1Δ*cph*-1Δ hyphal mutant. Studies have shown that neutrophils
355 respond to *C. albicans* site of entry, responding to epithelial-released cytokines and chemokines
356 in addition to recognizing fungal factors such as SAPs [85-88]. Neutrophils are able to phagocytize
357 and kill yeast cells and short hyphae while large hyphae are killed by inducing neutrophil
358 extracellular traps (NETs), which releases DNA, granule enzymes, and antimicrobial peptides [85,88-
359 91]. Furthermore, it has been shown that neutropenic patients developed candidemia from
360 candiduria, suggesting that bladder recruited neutrophils are critical to control fungal systemic
361 dissemination[59]. Our future studies will be focused on understanding the immune cell strategies
362 against the fungal CAUTI and their role in containing the fungal infection in the bladder.

363 *C. albicans* occupies many niches in the human body, and morphological changes are
364 associated with the establishment of diseased states. This is most important in the bladder, since it
365 is an open and dynamic system, where urine is constantly passing through. Therefore, in order to
366 establish a successful colonization, adhesion and biofilm formation on the urinary catheter is
367 essential[13,34,36,39,92]. Our results are consistent with that, *Candida* biofilms not only ensures
368 colonization but can protect the growing cells from the hostile environment and potentiate
369 establishment of the infection[93,94]. Targeting these hyphal genes so filamentation cannot occur
370 could be a possible therapeutic avenue for preventing *C. albicans* CAUTIs. Moreover, our results

bioRxiv preprint doi: https://doi.org/10.1101/2021.06.01.446547; this version posted June 2, 2021. The copyright holder for this preprint (which was not certified by peer review) is the author/funder, who has granted bioRxiv a license to display the preprint in perpetuity. It is made available under aCC-BY 4.0 International license.

highlight the importance of Fg and fibrin in the process, hence blocking deposition of these proteins onto the catheter might prevent fungal biofilm formation as well. As these fungal pathogens are becoming more commonplace in the healthcare setting, it is essential that the pathogenesis of *Candida spp.* is better understood in order to decrease the spread of infection and mortality rates. Understanding key characteristics of *C. albicans'* for CAUTI pathogenesis is the foundation to understanding and subsequently preventing *Candida spp.* infections.

MATERIALS AND METHODS

Ethics statement

All animal care was consistent with the Guide for the Care and Use of Laboratory Animals from the National Research Council. The University of Notre Dame Institutional Animal Care and Use Committee approved all mouse infections and procedures as part of protocol number 18-08-4792MD. For urine collections, all donors signed an informed consent form and protocols were approved by the Institutional Review Board of the University of Notre Dame under study #19-04-5273.

Urine Collection. Human urine from at least two healthy female donors between the ages of 20 - 35 were collected and pooled. Donors did not have a history of kidney disease, diabetes, or recent antibiotic treatment. Urine was sterilized with a 0.22 μm filter (VWR 29186-212) and pH was normalized to 6.0-6.5. BSA (VWR 97061-48) supplemented urine was sterilized again using a

bioRxiv preprint doi: https://doi.org/10.1101/2021.06.01.446547; this version posted June 2, 2021. The copyright holder for this preprint (which was not certified by peer review) is the author/funder, who has granted bioRxiv a license to display the preprint in perpetuity. It is made available under aCC-BY 4.0 International license.

393 0.22 μm filter. When urine was supplemented with Fg (Enzyme Research Laboratories FIB 3), it
394 was added directly to the sterilized urine and the urine was not sterilized after the addition of Fg.
395
396 **Fungal Culture Conditions.** All strains of *Candida albicans* were cultured at 37 °C with aeration
397 in 5 mL of YPD (10g/L Yeast Extract (VWR J850-500G), 20g/L Peptone (VWR J636-500G), 20
398 g/L Dextrose (VWR BDH9230-500G)) broth. For *in vivo* mouse experiments, *C. albicans* strains
399 were grown static for ~5 hrs in 5 mL of YPD followed by static overnight culture in human urine.
400
401 **Growth Curve.** Growth curves were performed in glass test tubes (Thermo Fisher Scientific 14-
402 961-29). Overnight cultures (all in stationary phase; measured using a UV/Vis Spectrophotometer)
403 were normalized to ~$1x10^7$ CFU/ml in 1xPBS (Sigma–Aldrich 1002786391). The culture was then
404 diluted (1:1000) into human urine (supplemented with 1 mg/mL BSA, 1 mg/mL Fg, 50X amino
405 acids, or 1 mg/mL human serum), BHI (incubated statically or shaking), or YPD (incubated
406 statically or shaking) and were incubated in the test tube at 37ºC for 48 hours. At 0, 24, and 48
407 hours, samples of each condition were taken and analyzed by CFU counts. All serum donors signed
408 an informed consent form and protocols were approved by the Institutional Review Board of the
409 University of Notre Dame under study #18-08-4834.
410
411 **Morphology Assay and CellProfiler Analysis.** All strains of *C. albicans* were grown in YPD
412 with or without serum and in human urine with or without serum. At 0, 24, and 48 hours, a sample
413 of each condition was taken, fixed with 10% formalin, and stained with 100 μg/mL of calcofluor.
414 Samples were viewed under a Zeiss inverted light microscope (Carl Zeiss, Thornwood, NY) with
415 the DAPI fluorescent channel. Random images were taken at 100x magnification and processed

bioRxiv preprint doi: https://doi.org/10.1101/2021.06.01.446547; this version posted June 2, 2021. The copyright holder for this preprint (which was not certified by peer review) is the author/funder, who has granted bioRxiv a license to display the preprint in perpetuity. It is made available under aCC-BY 4.0 International license.

with CellProfiler. A pipeline (CellProfiler) was created to identify fungal cells and measure the form factor (circularity) of each outlined cell. Based on the form factor value (form factor of a straight line is 0 and form factor of a perfect circle is 1), each cell was assigned to a particular morphology as follows: form factors <0.25, hypha; 0.25 – 0.5, pseudohypha; >0.5, yeast. Details on the pipeline are provided as supplementary materials. Images (consisting of a 3 x 3 tiled region, i.e. 9 fields of view) were randomly acquired and at least three images were analyzed per condition. The total number of cells per phenotype were summed and divided by the total number of cells to give the overall percentage of each cell type on Microsoft Excel.

Antibodies and dyes used in this study.

Primary antibodies: Goat anti-fibrinogen (Sigma-Aldrich F8512), rabbit anti-*Candida* (ThermoFisher Scientific PA1-27158), and rat anti-mouse Ly6G (BD Pharmingen 551459). **Secondary antibodies**: Alexaflour 488-labeled donkey anti-goat (ThermoFisher Scientific SA5-10086); Alexaflour 594-labeled donkey anti-rabbit (ThermoFisher Scientific SA5-10039); Alexaflour 647-labeled donkey anti-rat (ThermoFisher Scientific SA5-10029); IRDye 800CW donkey anti-goat; and IRDye 680LT donkey anti-rabbit. Alexaflour secondary antibodies were purchased from Invitrogen Molecular Probes and IRDye conjugates secondary antibodies from LI-COR Biosciences. **Dyes:** Hoechst dye (Thermo Fisher Scientific 62249) staining; Hematoxylin and Eosin (H&E) (vector Laboratories #H-3502).

Biofilm Formation in 96-well plates. Biofilm formations were performed in 96 well flat-bottomed plates (VWR 10861-562) were coated with 100uL of BSA or Fg (150 µg/mL) incubated

bioRxiv preprint doi: https://doi.org/10.1101/2021.06.01.446547; this version posted June 2, 2021. The copyright holder for this preprint (which was not certified by peer review) is the author/funder, who has granted bioRxiv a license to display the preprint in perpetuity. It is made available under aCC-BY 4.0 International license.

overnight at 4°C. The various strains were grown as described above and the inoculum normalized to ~1x10^6 CFU/ml. Cultures were then diluted (1:1000) into YPD, BHI, or human urine. 100uL of the inoculum were incubated in the wells of the 96 well plate at 37ºC for 48 hours while static.

Following the 48hr incubation, the supernatant was removed from the plate and washed three times with 200uL 1x PBS to remove unbound fungi. Plates were fixed with 10% neutralizing formalin (Leica 3800600) for 20 minutes and followed by three washes with PBS containing 0.05% Tween-20 (PBS-T). Blocking solution (PBS with 1.5% BSA and 0.1% sodium azide (Acros Organics 447811000)) was added to the plate for one hour at room temperature and then washed with PBS-T (3x). Biofilms were incubated with anti-*Candida* antibodies diluted into dilution buffer (PBS with 0.05% Tween (VWR M147-1L), 0.1% BSA) for two hours. Plates were washed three times with PBS-T and incubated for one hour with IRDye 680 LT donkey anti-rabbit secondary antibody solution at room temperature and washed with PBS-T (3x). As a final step, the biofilms were visualized by scanning the plates using the Odyssey Imaging System (LI-COR Biosciences) and the analyzed with Image Studio software to obtain the fluorescence intensities (LI-COR Version 5.2, Lincoln, NE).

BSA or Fg-coated dishes and formation of Fibrin fibers/nets. For these assays No. 0 coverglass glass-bottom 35 mm petri dish with a 14 mm microwell (MatTek P35G-0-14-C) were used. The dishes were coated with 150 µg/mL of BSA or Fg overnight at 4°C. For fibrin fiber/nets formation, Fg and thrombin (Sigma-Aldrich T6884-250UN) were thawed at 37°C. 100 µl of 0.5 mg/ml Fg in PBS was added into the microwell glass-bottom and then 10 µl of 2 U/ml thrombin was added to polymerize Fg into fibrin. Dishes were incubated at 37°C for 1 hour and kept overnight at 4°C

bioRxiv preprint doi: https://doi.org/10.1101/2021.06.01.446547; this version posted June 2, 2021. The copyright holder for this preprint (which was not certified by peer review) is the author/funder, who has granted bioRxiv a license to display the preprint in perpetuity. It is made available under aCC-BY 4.0 International license.

462 **Visualization of biofilms and fungal-fibrin interaction.** The various strains were grown as
463 described above and the inoculum normalized to ~1x10^7 CFU/ml in PBS. These cultures were then
464 diluted (1:1000) into human urine, added to the BSA-, Fg-, or fibrin coated dishes and then were
465 incubated at 37ºC for 48 hours under static conditions. After incubation, dishes were then washed
466 three times with 1x PBS to remove unbound fungi, then dishes were fixed with 10% neutralizing
467 formalin solution for 20 minutes and washed with 1x PBS three times. Dishes were blocked with
468 blocking solution was added for an hour at room temperature as described above. Then BSA- and
469 Fg-coated dishes were incubated in primary antibody (rabbit anti-*Candida*) and for fibrin-coated
470 dishes were incubated with rabbit anti-*Candida* and goat anti-Fg antibodies. Incubation with the
471 primary antibodies was done for two hours followed by three washes with PBS-T. Then, dishes
472 were incubated for 1 hour with Alexaflour 594-labeled donkey anti-rabbit secondary antibody for
473 BSA- and Fg-coated dishes and Alexaflour 594-labeled donkey anti-rabbit and Alexaflour 488-
474 labeled donkey anti-goat antibodies for fibrin-coated dishes, followed by three washes with PBS-
475 T. BSA- and Fg- coated dishes were visualized with a Zeiss inverted light microscope, and images
476 were taken at different magnifications (10x, 20x, 40x and 100x). Zen Pro and Fiji-ImageJ[95]
477 softwares were used to analyze the images. For the fungal-fibrin interaction, fibrin-coated dishes
478 were visualized by Nikon A1-R/Multi-Photon Laser Scanning Confocal Microscope and images
479 were analyzed by IMARIS Image Analysis software and ImageJ software[95].
480
481 ***In Vivo* Mouse Model.** Mice used in this study were ~6-week-old female wild-type C57BL/6 mice
482 purchased from Jackson Laboratory. Mice were subjected to transurethral implantation of a
483 silicone catheter and inoculated as previously described[57]. Briefly, mice were anesthetized by
484 inhalation of isoflurane and implanted with a 6-mm-long silicone catheter (BrainTree Scientific

bioRxiv preprint doi: https://doi.org/10.1101/2021.06.01.446547; this version posted June 2, 2021. The copyright holder for this preprint (which was not certified by peer review) is the author/funder, who has granted bioRxiv a license to display the preprint in perpetuity. It is made available under aCC-BY 4.0 International license.

SIL 025). Mice were infected immediately following catheter implantation with 50 µl of ~1×10^7 CFU/mL in PBS, of one of the fungal strains introduced into the bladder lumen by transurethral inoculation. Mice were sacrificed at 24 hours post infection by cervical dislocation after anesthesia inhalation and catheter, bladder, kidneys, spleen and heart were aseptically harvested for fungal CFU enumeration. A subset of catheters were fixed for imaging as described below and a subset of bladders were fixed and processed for immunofluorescence and histology analysis as described below.

Catheter Imaging and Analysis. Harvested catheters were fixed for imaging via standard IF procedure as previously described[54]. Briefly, catheters were fixed with formalin, blocked, washed with 1x PBS, and incubated with the appropriate primary antibodies overnight. Catheters were then incubated with secondary antibodies for two hours at room temperature. Catheters were washed with PBS-T and then a final wash with PBS. Catheters were visualized with the Odyssey Imaging System and then analyzed using color pixel counter from Fiji-ImageJ software[95]. The number of pixels of each color was compared to the total number of pixels to identify percent coverage of the catheter.

Bladder IHC and H&E Staining of Mouse Bladders. Mouse bladders were fixed in 10% formalin overnight, before being processed for sectioning and staining as previously described[53]. Briefly, bladder sections were deparaffinized, rehydrated, and rinsed with water. Antigen retrieval was accomplished by boiling the samples in Na-citrate, washing in tap water, and then incubating in 1x PBS three times. Sections were then blocked (1% BSA, 0.3% TritonX100 (Acros Organics 21568-2500) in 1x PBS) washed in 1x PBS, and incubated with appropriate primary antibodies diluted in blocking buffer overnight at 4 °C. Next, sections were washed with 1x PBS, incubated

bioRxiv preprint doi: https://doi.org/10.1101/2021.06.01.446547; this version posted June 2, 2021. The copyright holder for this preprint (which was not certified by peer review) is the author/funder, who has granted bioRxiv a license to display the preprint in perpetuity. It is made available under aCC-BY 4.0 International license.

with secondary antibodies for 2 h at room temperature, and washed once more in 1x PBS prior to Hoechst dye staining. Secondary antibodies for immunohistochemistry were Alexa 488 donkey anti-goat, Alexa 550 donkey anti-rabbit, and Alexa 650 donkey anti-rat. Hematoxylin and Eosin (H&E) stain for light microscopy was done by the CORE facilities at the University of Notre Dame (ND CORE). All imaging was done using a Zeiss inverted light microscope. Zen Pro and ImageJ software were used to analyze the images.

Statistical Analysis. Data from at least 3 experiments were pooled for each assay. Two-tailed Mann-Whitney *U* tests were performed with GraphPad Prism 5 software (GraphPad Software, San Diego, CA) for all comparisons described in biofilm, CAUTI, and catheter coverage experiments. Values represent means ± SEM derived from at least 3 independent experiments. *, $P<0.05$; **, $P<0.005$; ***, $P<0.0005$; ns, difference not significant.

bioRxiv preprint doi: https://doi.org/10.1101/2021.06.01.446547; this version posted June 2, 2021. The copyright holder for this preprint (which was not certified by peer review) is the author/funder, who has granted bioRxiv a license to display the preprint in perpetuity. It is made available under aCC-BY 4.0 International license.

REFERENCES

1 Flores-Mireles, A., Hreha, T. N. & Hunstad, D. A. Pathophysiology, Treatment, and Prevention of Catheter-Associated Urinary Tract Infection. *Top Spinal Cord Inj Rehabil* **25**, 228-240, doi:10.1310/sci2503-228 (2019).

2 Fisher, J. F., Kavanagh, K., Sobel, J. D., Kauffman, C. A. & Newman, C. A. Candida urinary tract infection: pathogenesis. *Clin Infect Dis* **52 Suppl 6**, S437-451, doi:10.1093/cid/cir110 (2011).

3 R, Y., M, P. S., U, A. B., R, R. & K, B. A. Candiduria: prevalence and trends in antifungal susceptibility in a tertiary care hospital of mangalore. *J Clin Diagn Res* **7**, 2459-2461, doi:10.7860/jcdr/2013/6298.3578 (2013).

4 Casanova, M. *et al.* Identification of a 58-kilodalton cell surface fibrinogen-binding mannoprotein from Candida albicans. *Infect Immun* **60**, 4221-4229 (1992).

5 Flores-Mireles, A. L. *et al.* Fibrinogen Release and Deposition on Urinary Catheters Placed during Urological Procedures. *J Urol* **196**, 416-421, doi:10.1016/j.juro.2016.01.100 (2016).

6 Pfaller, M. A. & Diekema, D. J. Epidemiology of invasive candidiasis: a persistent public health problem. *Clin Microbiol Rev* **20**, 133-163, doi:10.1128/cmr.00029-06 (2007).

7 Rodrigues, M. L. & Nosanchuk, J. D. Fungal diseases as neglected pathogens: A wake-up call to public health officials. *PLoS Negl Trop Dis* **14**, e0007964, doi:10.1371/journal.pntd.0007964 (2020).

8 Sanguinetti, M., Posteraro, B. & Lass-Flörl, C. Antifungal drug resistance among Candida species: mechanisms and clinical impact. *Mycoses* **58 Suppl 2**, 2-13, doi:10.1111/myc.12330 (2015).

9 Antibiotic resistance threats in the United States, 2019. (2019).

10 Nobile, C. J. & Johnson, A. D. Candida albicans Biofilms and Human Disease. *Annu Rev Microbiol* **69**, 71-92, doi:10.1146/annurev-micro-091014-104330 (2015).

11 Tsui, C., Kong, E. F. & Jabra-Rizk, M. A. Pathogenesis of Candida albicans biofilm. *Pathog Dis* **74**, ftw018, doi:10.1093/femspd/ftw018 (2016).

12 Duggan, S., Leonhardt, I., Hunniger, K. & Kurzai, O. Host response to Candida albicans bloodstream infection and sepsis. *Virulence* **6**, 316-326, doi:10.4161/21505594.2014.988096 (2015).

13 Flores-Mireles, A. L., Walker, J. N., Caparon, M. & Hultgren, S. J. Urinary tract infections: epidemiology, mechanisms of infection and treatment options. *Nat Rev Microbiol* **13**, 269-284, doi:10.1038/nrmicro3432 (2015).

14 Maki, D. G. & Tambyah, P. A. Engineering out the risk for infection with urinary catheters. *Emerg Infect Dis* **7**, 342-347, doi:10.3201/eid0702.010240 (2001).

15 Rogers, M. A. *et al.* Use of urinary collection devices in skilled nursing facilities in five states. *J Am Geriatr Soc* **56**, 854-861, doi:10.1111/j.1532-5415.2008.01675.x (2008).

16 Montoya, A. & Mody, L. Common infections in nursing homes: a review of current issues and challenges. *Aging health* **7**, 889-899, doi:10.2217/ahe.11.80 (2011).

17 Cleary, I. A. *et al.* Examination of the pathogenic potential of Candida albicans filamentous cells in an animal model of haematogenously disseminated candidiasis. *FEMS Yeast Res* **16**, fow011, doi:10.1093/femsyr/fow011 (2016).

18 Mayer, F. L., Wilson, D. & Hube, B. Candida albicans pathogenicity mechanisms. *Virulence* **4**, 119-128, doi:10.4161/viru.22913 (2013).

19 Thompson, D. S., Carlisle, P. L. & Kadosh, D. Coevolution of morphology and virulence in Candida species. *Eukaryot Cell* **10**, 1173-1182, doi:10.1128/EC.05085-11 (2011).

20 Sudbery, P. E. Growth of Candida albicans hyphae. *Nat Rev Microbiol* **9**, 737-748, doi:10.1038/nrmicro2636 (2011).

bioRxiv preprint doi: https://doi.org/10.1101/2021.06.01.446547; this version posted June 2, 2021. The copyright holder for this preprint (which was not certified by peer review) is the author/funder, who has granted bioRxiv a license to display the preprint in perpetuity. It is made available under aCC-BY 4.0 International license.

21 Noble, S. M., Gianetti, B. A. & Witchley, J. N. Candida albicans cell-type switching and functional plasticity in the mammalian host. *Nat Rev Microbiol* **15**, 96-108, doi:10.1038/nrmicro.2016.157 (2017).

22 Pukkila-Worley, R., Peleg, A. Y., Tampakakis, E. & Mylonakis, E. Candida albicans Hyphal Formation and Virulence Assessed Using a Caenorhabditis elegans Infection Model. *Eukaryotic Cell* **8**, 1750-1758, doi:10.1128/Ec.00163-09 (2009).

23 Maddirala, A. R. *et al.* Biphenyl Gal and GalNAc FmlH Lectin Antagonists of Uropathogenic E. coli (UPEC): Optimization through Iterative Rational Drug Design. *J Med Chem* **62**, 467-479, doi:10.1021/acs.jmedchem.8b01561 (2019).

24 Nett, J. E. & Andes, D. R. Contributions of the Biofilm Matrix to Candida Pathogenesis. *J Fungi (Basel)* **6**, doi:10.3390/jof6010021 (2020).

25 Wall, G., Montelongo-Jauregui, D., Vidal Bonifacio, B., Lopez-Ribot, J. L. & Uppuluri, P. Candida albicans biofilm growth and dispersal: contributions to pathogenesis. *Curr Opin Microbiol* **52**, 1-6, doi:10.1016/j.mib.2019.04.001 (2019).

26 Coste, A. T. *et al.* Emerging echinocandin-resistant Candida albicans and glabrata in Switzerland. *Infection* **48**, 761-766, doi:10.1007/s15010-020-01475-8 (2020).

27 Pristov, K. E. & Ghannoum, M. A. Resistance of Candida to azoles and echinocandins worldwide. *Clinical Microbiology and Infection* **25**, 792-798, doi:https://doi.org/10.1016/j.cmi.2019.03.028 (2019).

28 Fisher, J. F., Sobel, J. D., Kauffman, C. A. & Newman, C. A. Candida urinary tract infections--treatment. *Clin Infect Dis* **52 Suppl 6**, S457-466, doi:10.1093/cid/cir112 (2011).

29 O'Brien, V. P., Hannan, T. J., Nielsen, H. V. & Hultgren, S. J. Drug and Vaccine Development for the Treatment and Prevention of Urinary Tract Infections. *Microbiology spectrum* **4**, doi:10.1128/microbiolspec.UTI-0013-2012 (2016).

30 Garibaldi, R. A., Burke, J. P., Dickman, M. L. & Smith, C. B. Factors predisposing to bacteriuria during indwelling urethral catheterization. *The New England journal of medicine* **291**, 215-219, doi:10.1056/NEJM197408012910501 (1974).

31 Norden, C. W., Green, G. M. & Kass, E. H. Antibacterial mechanisms of the urinary bladder. *The Journal of clinical investigation* **47**, 2689-2700, doi:10.1172/JCI105952 (1968).

32 Warren, J. W. Catheter-associated urinary tract infections. *Infectious disease clinics of North America* **11**, 609-622 (1997).

33 Parsons, C. L. Pathogenesis of urinary tract infections. Bacterial adherence, bladder defense mechanisms. *The Urologic clinics of North America* **13**, 563-568 (1986).

34 Flores-Mireles, A. L., Pinkner, J. S., Caparon, M. G. & Hultgren, S. J. EbpA vaccine antibodies block binding of Enterococcus faecalis to fibrinogen to prevent catheter-associated bladder infection in mice. *Sci Transl Med* **6**, 254ra127, doi:10.1126/scitranslmed.3009384 (2014).

35 Flores-Mireles, A. L. *et al.* Antibody-Based Therapy for Enterococcal Catheter-Associated Urinary Tract Infections. *Mbio* **7**, doi:10.1128/mBio.01653-16 (2016).

36 Flores-Mireles, A. L. *et al.* Antibody-Based Therapy for Enterococcal Catheter-Associated Urinary Tract Infections. *Mbio* **7**, doi:ARTN e01653-1610.1128/mBio.01653-16 (2016).

37 Guiton, P. S., Hannan, T. J., Ford, B., Caparon, M. G. & Hultgren, S. J. Enterococcus faecalis overcomes foreign body-mediated inflammation to establish urinary tract infections. *Infect Immun* **81**, 329-339, doi:10.1128/IAI.00856-12 (2013).

38 Guiton, P. S., Hung, C. S., Hancock, L. E., Caparon, M. G. & Hultgren, S. J. Enterococcal biofilm formation and virulence in an optimized murine model of foreign body-associated urinary tract infections. *Infect Immun* **78**, 4166-4175, doi:10.1128/IAI.00711-10 (2010).

bioRxiv preprint doi: https://doi.org/10.1101/2021.06.01.446547; this version posted June 2, 2021. The copyright holder for this preprint (which was not certified by peer review) is the author/funder, who has granted bioRxiv a license to display the preprint in perpetuity. It is made available under aCC-BY 4.0 International license.

39 Walker, J. N. *et al.* Catheterization alters bladder ecology to potentiate Staphylococcus aureus infection of the urinary tract. *Proc Natl Acad Sci U S A* **114**, E8721-E8730, doi:10.1073/pnas.1707572114 (2017).

40 Di Venanzio, G. *et al.* Urinary tract colonization is enhanced by a plasmid that regulates uropathogenic Acinetobacter baumannii chromosomal genes. *Nat Commun* **10**, doi:ARTN 276310.1038/s41467-019-10706-y (2019).

41 Gaston, J. R. *et al.* Enterococcus faecalis Polymicrobial Interactions Facilitate Biofilm Formation, Antibiotic Recalcitrance, and Persistent Colonization of the Catheterized Urinary Tract. *Pathogens* **9**, doi:ARTN 83510.3390/pathogens9100835 (2020).

42 Alves, R. *et al.* Adapting to survive: How Candida overcomes host-imposed constraints during human colonization. *Plos Pathog* **16**, doi:ARTN e100847810.1371/journal.ppat.1008478 (2020).

43 Walker, J. N. *et al.* High-resolution imaging reveals microbial biofilms on patient urinary catheters despite antibiotic administration. *World J Urol* **38**, 2237-2245, doi:10.1007/s00345-019-03027-8 (2020).

44 Bar-Yosef, H., Vivanco Gonzalez, N., Ben-Aroya, S., Kron, S. J. & Kornitzer, D. Chemical inhibitors of Candida albicans hyphal morphogenesis target endocytosis. *Sci Rep* **7**, 5692, doi:10.1038/s41598-017-05741-y (2017).

45 Watanabe, H., Azuma, M., Igarashi, K. & Ooshima, H. Relationship between cell morphology and intracellular potassium concentration in Candida albicans. *J Antibiot* **59**, 281-287, doi:DOI 10.1038/ja.2006.39 (2006).

46 Feng, Q. H., Summers, E., Guo, B. & Fink, G. Ras signaling is required for serum-induced hyphal differentiation in Candida albicans. *Journal of Bacteriology* **181**, 6339-6346, doi:Doi 10.1128/Jb.181.20.6339-6346.1999 (1999).

47 Kamentsky, L. *et al.* Improved structure, function and compatibility for CellProfiler: modular high-throughput image analysis software. *Bioinformatics* **27**, 1179-1180, doi:10.1093/bioinformatics/btr095 (2011).

48 Nett, J. E. *et al.* Rat indwelling urinary catheter model of Candida albicans biofilm infection. *Infect Immun* **82**, 4931-4940, doi:10.1128/IAI.02284-14 (2014).

49 Nett, J. E. *et al.* Host contributions to construction of three device-associated Candida albicans biofilms. *Infect Immun* **83**, 4630-4638, doi:10.1128/IAI.00931-15 (2015).

50 Schaller, M., Borelli, C., Korting, H. C. & Hube, B. Hydrolytic enzymes as virulence factors of Candida albicans. *Mycoses* **48**, 365-377, doi:10.1111/j.1439-0507.2005.01165.x (2005).

51 Carlisle, P. L. *et al.* Expression levels of a filament-specific transcriptional regulator are sufficient to determine Candida albicans morphology and virulence. *P Natl Acad Sci USA* **106**, 599-604, doi:10.1073/pnas.0804061106 (2009).

52 Sepulveda, P. *et al. Candida albicans* fibrinogen binding mannoprotein: expression in clinical strains and immunogenicity in patients with candidiasis. *International microbiology : the official journal of the Spanish Society for Microbiology* **1**, 209-216 (1998).

53 Walker, J. N. *et al.* Catheterization alters bladder ecology to potentiate Staphylococcus aureus infection of the urinary tract. *P Natl Acad Sci USA* **114**, E8721-E8730, doi:10.1073/pnas.1707572114 (2017).

54 Colomer-Winter, C., Lemos, J. A. & Flores-Mireles, A. L. Biofilm Assays on Fibrinogen-coated Silicone Catheters and 96-well Polystyrene Plates. *Bio Protoc* **9**, doi:10.21769/BioProtoc.3196 (2019).

55 Colomer-Winter, C. *et al.* Manganese acquisition is essential for virulence of Enterococcus faecalis. *Plos Pathog* **14**, e1007102, doi:10.1371/journal.ppat.1007102 (2018).

bioRxiv preprint doi: https://doi.org/10.1101/2021.06.01.446547; this version posted June 2, 2021. The copyright holder for this preprint (which was not certified by peer review) is the author/funder, who has granted bioRxiv a license to display the preprint in perpetuity. It is made available under aCC-BY 4.0 International license.

56 Colomer-Winter, C., Flores-Mireles, A. L., Kundra, S., Hultgren, S. J. & Lemos, J. A. (p)ppGpp and CodY Promote Enterococcus faecalis Virulence in a Murine Model of Catheter-Associated Urinary Tract Infection. *mSphere* **4**, doi:10.1128/mSphere.00392-19 (2019).

57 Conover, M. S., Flores-Mireles, A. L., Hibbing, M. E., Dodson, K. & Hultgren, S. J. Establishment and Characterization of UTI and CAUTI in a Mouse Model. *J Vis Exp*, e52892, doi:10.3791/52892 (2015).

58 Peman, J. & Ruiz-Gaitan, A. Candidemia from urinary tract source: the challenge of candiduria. *Hosp Pract (1995)* **46**, 243-245, doi:10.1080/21548331.2018.1538623 (2018).

59 Pappas, P. G. *et al.* Clinical Practice Guideline for the Management of Candidiasis: 2016 Update by the Infectious Diseases Society of America. *Clin Infect Dis* **62**, e1-50, doi:10.1093/cid/civ933 (2016).

60 Huang, P. Y. *et al.* Molecular concordance of concurrent Candida albicans candidemia and candiduria. *Diagn Micr Infec Dis* **76**, 382-384, doi:10.1016/j.diagmicrobio.2013.03.015 (2013).

61 Kauffman, C. A. *et al.* Prospective multicenter surveillance study of funguria in hospitalized patients. *Clinical Infectious Diseases* **30**, 14-18, doi:Doi 10.1086/313583 (2000).

62 Rousseau, M. *et al.* Bladder catheterization increases susceptibility to infection that can be prevented by prophylactic antibiotic treatment. *Jci Insight* **1**, doi:ARTN e8817810.1172/jci.insight.88178 (2016).

63 Conway, L. J., Carter, E. J. & Larson, E. L. Risk Factors for Nosocomial Bacteremia Secondary to Urinary Catheter-Associated Bacteriuria: A Systematic Review. *Urol Nurs* **35**, 191-203 (2015).

64 Greene, M. T. *et al.* Predictors of hospital-acquired urinary tract-related bloodstream infection. *Infect Control Hosp Epidemiol* **33**, 1001-1007, doi:10.1086/667731 (2012).

65 Nicolle, L. E. Catheter associated urinary tract infections. *Antimicrob Resist Infect Control* **3**, 23, doi:10.1186/2047-2994-3-23 (2014).

66 Guiton, P. S. *et al.* Contribution of autolysin and Sortase a during Enterococcus faecalis DNA-dependent biofilm development. *Infect Immun* **77**, 3626-3638, doi:10.1128/IAI.00219-09 (2009).

67 Zarnowski, R. *et al.* Novel entries in a fungal biofilm matrix encyclopedia. *Mbio* **5**, e01333-01314, doi:10.1128/mBio.01333-14 (2014).

68 Dwivedi, P. *et al.* Role of Bcr1-activated genes Hwp1 and Hyr1 in Candida albicans oral mucosal biofilms and neutrophil evasion. *PLoS One* **6**, e16218, doi:10.1371/journal.pone.0016218 (2011).

69 Nobile, C. J., Nett, J. E., Andes, D. R. & Mitchell, A. P. Function of Candida albicans adhesin Hwp1 in biofilm formation. *Eukaryot Cell* **5**, 1604-1610, doi:10.1128/EC.00194-06 (2006).

70 Nobile, C. J. *et al.* Critical role of Bcr1-dependent adhesins in C. albicans biofilm formation in vitro and in vivo. *Plos Pathog* **2**, e63, doi:10.1371/journal.ppat.0020063 (2006).

71 Oh, S. H. *et al.* Agglutinin-Like Sequence (ALS) Genes in the Candida parapsilosis Species Complex: Blurring the Boundaries Between Gene Families That Encode Cell-Wall Proteins. *Frontiers in Microbiology* **10**, doi:ARTN 78110.3389/fmicb.2019.00781 (2019).

72 Hoyer, L. L. & Cota, E. Candida albicans Agglutinin-Like Sequence (Als) Family Vignettes: A Review of Als Protein Structure and Function. *Front Microbiol* **7**, 280, doi:10.3389/fmicb.2016.00280 (2016).

73 Hoyer, L. L., Green, C. B., Oh, S. H. & Zhao, X. Discovering the secrets of the Candida albicans agglutinin-like sequence (ALS) gene family--a sticky pursuit. *Med Mycol* **46**, 1-15, doi:10.1080/13693780701435317 (2008).

74 Salgado, P. S. *et al.* Structural basis for the broad specificity to host-cell ligands by the pathogenic fungus Candida albicans. *Proc Natl Acad Sci U S A* **108**, 15775-15779, doi:10.1073/pnas.1103496108 (2011).

75 Lin, J. *et al.* The peptide-binding cavity is essential for Als3-mediated adhesion of Candida albicans to human cells. *J Biol Chem* **289**, 18401-18412, doi:10.1074/jbc.M114.547877 (2014).

bioRxiv preprint doi: https://doi.org/10.1101/2021.06.01.446547; this version posted June 2, 2021. The copyright holder for this preprint (which was not certified by peer review) is the author/funder, who has granted bioRxiv a license to display the preprint in perpetuity. It is made available under aCC-BY 4.0 International license.

76 Nantel, A. *et al.* Transcription profiling of Candida albicans cells undergoing the yeast-to-hyphal transition. *Mol Biol Cell* **13**, 3452-3465, doi:10.1091/mbc.e02-05-0272 (2002).

77 Kadosh, D. & Johnson, A. D. Induction of the Candida albicans filamentous growth program by relief of transcriptional repression: a genome-wide analysis. *Mol Biol Cell* **16**, 2903-2912, doi:10.1091/mbc.e05-01-0073 (2005).

78 Carlisle, P. L. & Kadosh, D. A genome-wide transcriptional analysis of morphology determination in Candida albicans. *Mol Biol Cell* **24**, 246-260, doi:10.1091/mbc.E12-01-0065 (2013).

79 Witchley, J. N. *et al.* Candida albicans Morphogenesis Programs Control the Balance between Gut Commensalism and Invasive Infection. *Cell Host Microbe* **25**, 432-443 e436, doi:10.1016/j.chom.2019.02.008 (2019).

80 Felk, A. *et al.* Candida albicans hyphal formation and the expression of the Efg1-regulated proteinases Sap4 to Sap6 are required for the invasion of parenchymal organs. *Infect Immun* **70**, 3689-3700, doi:10.1128/iai.70.7.3689-3700.2002 (2002).

81 Leng, P., Lee, P. R., Wu, H. & Brown, A. J. Efg1, a morphogenetic regulator in Candida albicans, is a sequence-specific DNA binding protein. *J Bacteriol* **183**, 4090-4093, doi:10.1128/JB.183.13.4090-4093.2001 (2001).

82 Chandra, J. *et al.* Biofilm formation by the fungal pathogen Candida albicans: development, architecture, and drug resistance. *J Bacteriol* **183**, 5385-5394, doi:10.1128/jb.183.18.5385-5394.2001 (2001).

83 Nobile, C. J. & Mitchell, A. P. Regulation of cell-surface genes and biofilm formation by the C. albicans transcription factor Bcr1p. *Curr Biol* **15**, 1150-1155, doi:10.1016/j.cub.2005.05.047 (2005).

84 Heilmann, C. J. *et al.* Hyphal induction in the human fungal pathogen Candida albicans reveals a characteristic wall protein profile. *Microbiology (Reading)* **157**, 2297-2307, doi:10.1099/mic.0.049395-0 (2011).

85 Rubin-Bejerano, I., Fraser, I., Grisafi, P. & Fink, G. R. Phagocytosis by neutrophils induces an amino acid deprivation response in Saccharomyces cerevisiae and Candida albicans. *Proc Natl Acad Sci U S A* **100**, 11007-11012, doi:10.1073/pnas.1834481100 (2003).

86 Gabrielli, E. *et al.* In vivo induction of neutrophil chemotaxis by secretory aspartyl proteinases of Candida albicans. *Virulence* **7**, 819-825, doi:10.1080/21505594.2016.1184385 (2016).

87 Weindl, G. *et al.* Human epithelial cells establish direct antifungal defense through TLR4-mediated signaling. *The Journal of clinical investigation* **117**, 3664-3672, doi:10.1172/JCI28115 (2007).

88 Naglik, J. R., Konig, A., Hube, B. & Gaffen, S. L. Candida albicans-epithelial interactions and induction of mucosal innate immunity. *Curr Opin Microbiol* **40**, 104-112, doi:10.1016/j.mib.2017.10.030 (2017).

89 Urban, C. F., Reichard, U., Brinkmann, V. & Zychlinsky, A. Neutrophil extracellular traps capture and kill Candida albicans yeast and hyphal forms. *Cell Microbiol* **8**, 668-676, doi:10.1111/j.1462-5822.2005.00659.x (2006).

90 Urban, C. F. *et al.* Neutrophil extracellular traps contain calprotectin, a cytosolic protein complex involved in host defense against Candida albicans. *Plos Pathog* **5**, e1000639, doi:10.1371/journal.ppat.1000639 (2009).

91 Kenno, S., Perito, S., Mosci, P., Vecchiarelli, A. & Monari, C. Autophagy and Reactive Oxygen Species Are Involved in Neutrophil Extracellular Traps Release Induced by C. albicans Morphotypes. *Front Microbiol* **7**, 879, doi:10.3389/fmicb.2016.00879 (2016).

92 Nielsen, H. V. *et al.* Pilin and sortase residues critical for endocarditis- and biofilm-associated pilus biogenesis in Enterococcus faecalis. *J Bacteriol* **195**, 4484-4495, doi:10.1128/JB.00451-13 (2013).

bioRxiv preprint doi: https://doi.org/10.1101/2021.06.01.446547; this version posted June 2, 2021. The copyright holder for this preprint (which was not certified by peer review) is the author/funder, who has granted bioRxiv a license to display the preprint in perpetuity. It is made available under aCC-BY 4.0 International license.

93 Cavalheiro, M. & Teixeira, M. C. Candida Biofilms: Threats, Challenges, and Promising Strategies. *Front Med (Lausanne)* **5**, 28, doi:10.3389/fmed.2018.00028 (2018).

94 Flemming, H. C. *et al.* Biofilms: an emergent form of bacterial life. *Nat Rev Microbiol* **14**, 563-575, doi:10.1038/nrmicro.2016.94 (2016).

95 Schindelin, J. *et al.* Fiji: an open-source platform for biological-image analysis. *Nat Methods* **9**, 676-682, doi:10.1038/nmeth.2019 (2012).

Acknowledgments We thank members of the A.L.F.M. and F.H.S.T. laboratories for their helpful suggestions and insightful comments. Especial thank you to Dr. Michael G. Caparon for his comments. **Funding:** This work was supported by institutional funds from the University of Notre Dame (to A.L.F.M. and F.H.S.T). **Author contributions** A.L.F.M., and F.H.S.T designed the experiments. A.L.L., M.J.A., A.M., P.S. performed the studies. A.L.L., A.L.F.M, and F.H.S.T. wrote the paper. **Competing interests:** The authors declare no competing financial interests.

bioRxiv preprint doi: https://doi.org/10.1101/2021.06.01.446547; this version posted June 2, 2021. The copyright holder for this preprint (which was not certified by peer review) is the author/funder, who has granted bioRxiv a license to display the preprint in perpetuity. It is made available under aCC-BY 4.0 International license.

Figures:

Figure 1. *C. albicans* grows and survives in urine. Growth curves of *C. albicans* Pt. 62 (A), Pt. 65 (B), PNCL1 (C), DAY230 (D), SC5314 (E), and SC5314 *efg-1*Δ*cph-1*Δ (F), grown in YPD, BHI, human urine conditions alone, or urine conditions supplemented with 3% human serum (serum), fibrinogen (Fg), bovine serum albumin (BSA), or amino acids (AA). Fungal growth was determined by CFUs enumeration after 0, 24, and 48 hours. Except when indicated, all strains were grown under static conditions. Data presented shows the mean and standard error derived from three independent experiments with five technical replicates.

Figure 2. Urine conditions prompt hyphal *C. albicans* to take on a morphology. The morphology of *C. albicans* strains were evaluated after 0, 24, and 48 hours of growth in urine and YPD with or without 3% human serum. Imaging of a population of ~300 cells/per field of view (at least 3 random field of views for each strain) were analyzed using CellProfiler to identify yeast cells and classify them based on the circularity (see Materials and Methods) of each cell as follows: hyphal (<0.25), pseudohyphal (0.25 – 0.5), or yeast (>0.5) (G).

Figure 3. Fibrinogen enhances *C. albicans'* biofilm formation. (A-F) Immunostaining analysis of biofilm formation on BSA- or Fg- coated microplates by *C. albicans* strains when grown in YPD, BHI, or human urine. At 48 hrs, *C. albicans'* biofilm was measured by fluorescence intensity by using anti-*Candida* antibodies. Data presented shows the mean and standard error derived from three independent experiments with 24 technical replicates. Differences between groups were tested for significance using the Mann-Whitney U test. ****, P<0.0001; ns, not statistically

bioRxiv preprint doi: https://doi.org/10.1101/2021.06.01.446547; this version posted June 2, 2021. The copyright holder for this preprint (which was not certified by peer review) is the author/funder, who has granted bioRxiv a license to display the preprint in perpetuity. It is made available under aCC-BY 4.0 International license.

different. (G-L) Microscopically visualization of 48 hrs *C. albicans'* biofilms biomass on BSA- or Fg-coated glass bottom petri dishes grown in urine using anti-*Candida* antibodies.

Figure 4. *C. albicans*-interaction with fibrin fibers/nets in urine conditions. (A-F) Microscopically visualization and 3D reconstruction of 48 hrs *C. albicans'* biofilms on fibrin fibers/nets grown in human urine using antibodies against Fg (anti-Fg; green) and *C. albicans* (anti–Candida; red). Scale bars: 100 μm for 10x and 500 μm for 40x. White squares represent the zoom-in area used for the higher magnification (x).

Figure 5. *In vivo* infection shows hyphal formation is required for CAUTI. Mice were implanted with catheters and infected with 1 x 10^6 CFU of one of the six *C. albicans* strains. After 24 hours, the organs (bladder, kidneys, spleen, and heart) and catheter were recovered and subjected to analysis by CFUs. (**A-D**) Mice experienced a high fungal burden on the harvested organs and catheter. (**E**) Mice infected with SC5314 *efg-1*Δ*cph-1*Δ showed significantly less colonization of the bladder, catheter, and kidneys as opposed to the SC5314 WT strain. Values represent means ± SEM. The Mann-Whitney U test was used; *, $P < 0.05$ was considered statistically significant. **, $P < 0.005$; ns, values were not statistically significantly different. The horizontal bar represents the median value. The horizontal broken line represents the limit of detection of viable bacteria. LOD; limit of detection.

Figure 6. Hyphal *C. albicans* cells invade the lumen of the catheterized bladder. Mice were implanted and infected with 1x 10^6 CFU with the corresponding strain and at 24 hpi, bladders tissues and catheters were recovered. Bladder were subjected to analysis by H&E and IF staining. For the IF analysis antibody staining was used to detect Fg (anti-Fg; green), *C. albicans* (anti–

bioRxiv preprint doi: https://doi.org/10.1101/2021.06.01.446547; this version posted June 2, 2021. The copyright holder for this preprint (which was not certified by peer review) is the author/funder, who has granted bioRxiv a license to display the preprint in perpetuity. It is made available under aCC-BY 4.0 International license.

Candida; red), and neutrophils (anti-Ly6G; white). Antibody staining with DAPI (blue) delineated the urothelium and cell nuclei (representative images). The white broken line separates the bladder lumen (L) from the urothelium surface (U), the lamina propria (LP), and muscularis (M). H&E stained bladder scale bars, 700 µm. White squares represent a zoom in done for the next magnification (x). Blue arrow heads indicate *C. albicans* colonization.

Figure 7. Colocalization of *C. albicans* strains with deposited fibrinogen on catheters during CAUTI. Catheterized mice were challenged with $1x10^6$ CFU of the indicated *C. albicans* strain. Then implanted catheters were retrieved 24hpi stained with antibodies to detect Fg (anti-Fg; green) and *C. albicans* (anti-Candida; red) (**B-G**). Quantification of fungal colocalization with deposited Fg on the catheter (**H-L**). The Mann-Whitney U test was used to analyze catheter colonization between SC5314 WT and hyphal mutant; *, $P < 0.05$; Values represent the means ± standard deviation derived from co-localization of the catheter segments. Non-implanted catheters were used a negative control (**A**).

bioRxiv preprint doi: https://doi.org/10.1101/2021.06.01.446547; this version posted June 2, 2021. The copyright holder for this preprint (which was not certified by peer review) is the author/funder, who has granted bioRxiv a license to display the preprint in perpetuity. It is made available under aCC-BY 4.0 International license.

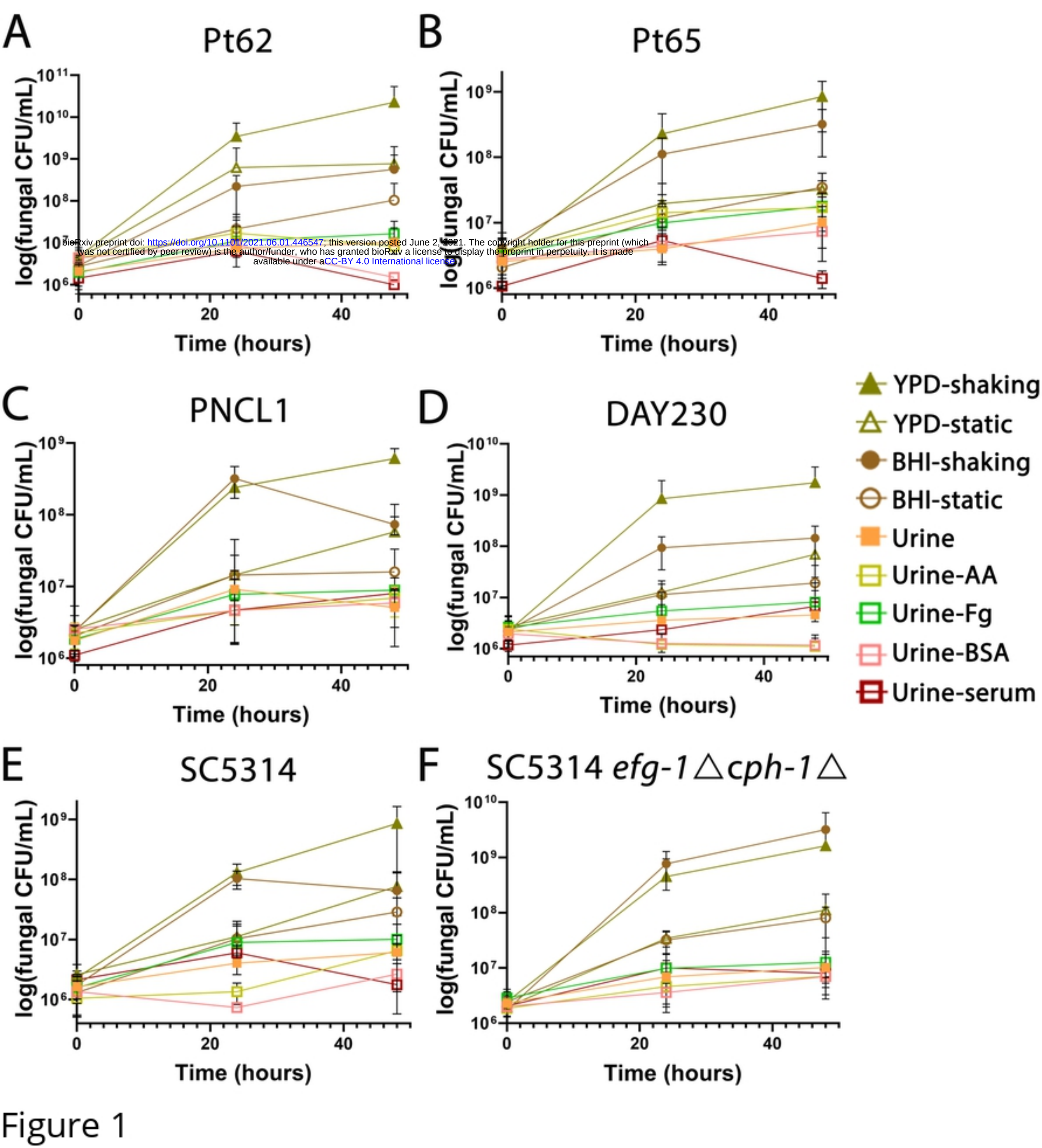

Figure 1

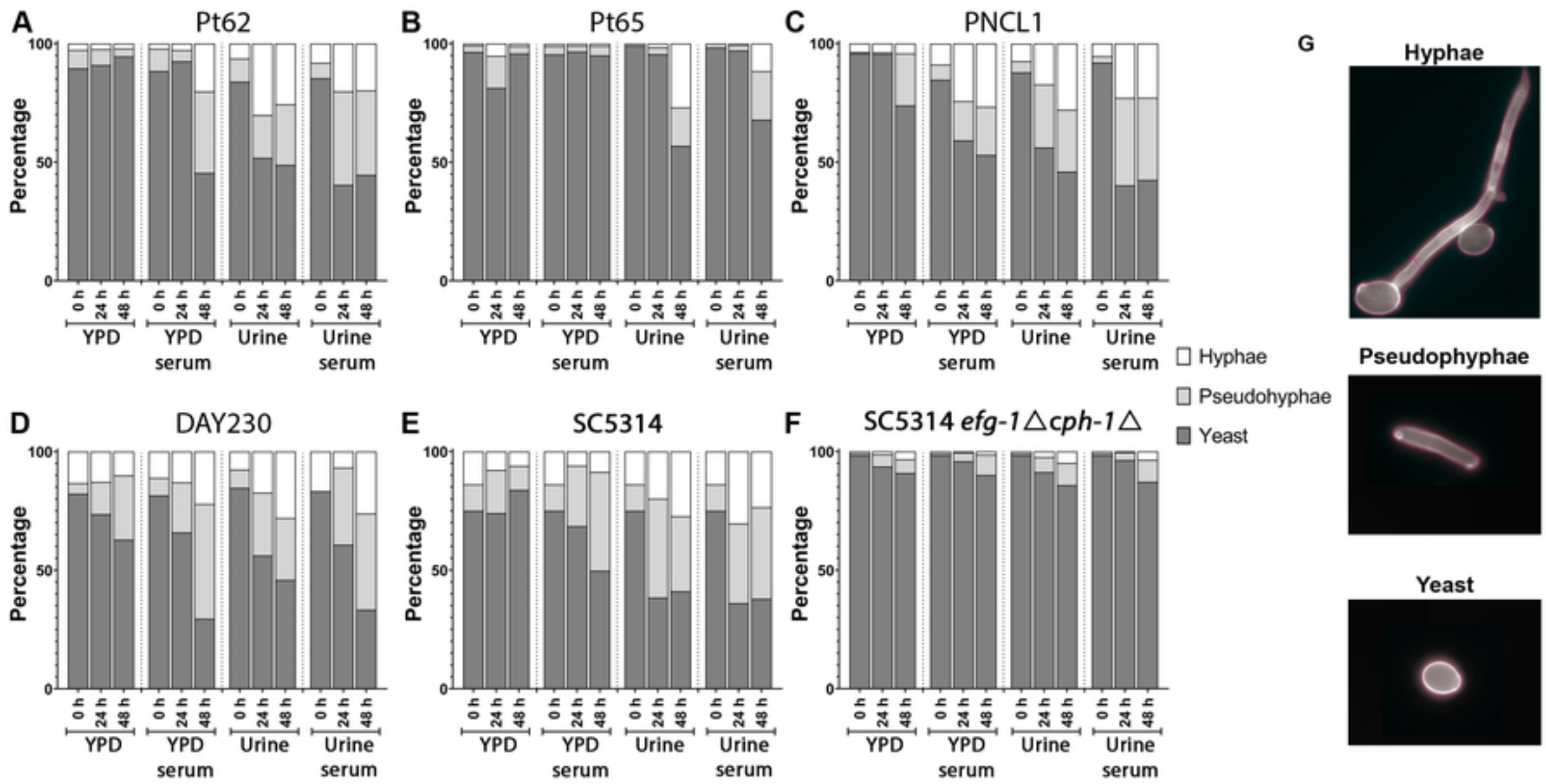
A
Pt62
B
Pt65
C
PNCL1
D
DAY230
E
SC5314
F
SC5314 efg-1△cph-1△
Percentage
100
50
0
0 h
24 h
48 h
YPD
YPD serum
Urine
Urine serum
Hyphae
Pseudohyphae
Yeast
G
Hyphae
Pseudophyphae
Yeast

Figure 2

bioRxiv preprint doi: https://doi.org/10.1101/2021.06.01.446547 ight holder for this preprint (which
was not certified by peer review) is the author/funder, eprint in perpetuity. It is made
available u CC-BY 4.0 International license

Figure 3

bioRxiv preprint doi: https://doi.org/10.1101/2021.06.01.446547; this version posted June 2, 2021. The copyright holder for this preprint (which was not certified by peer review) is the author/funder, who has granted bioRxiv a license to display the preprint in perpetuity. It is made available under aCC-BY 4.0 International license.

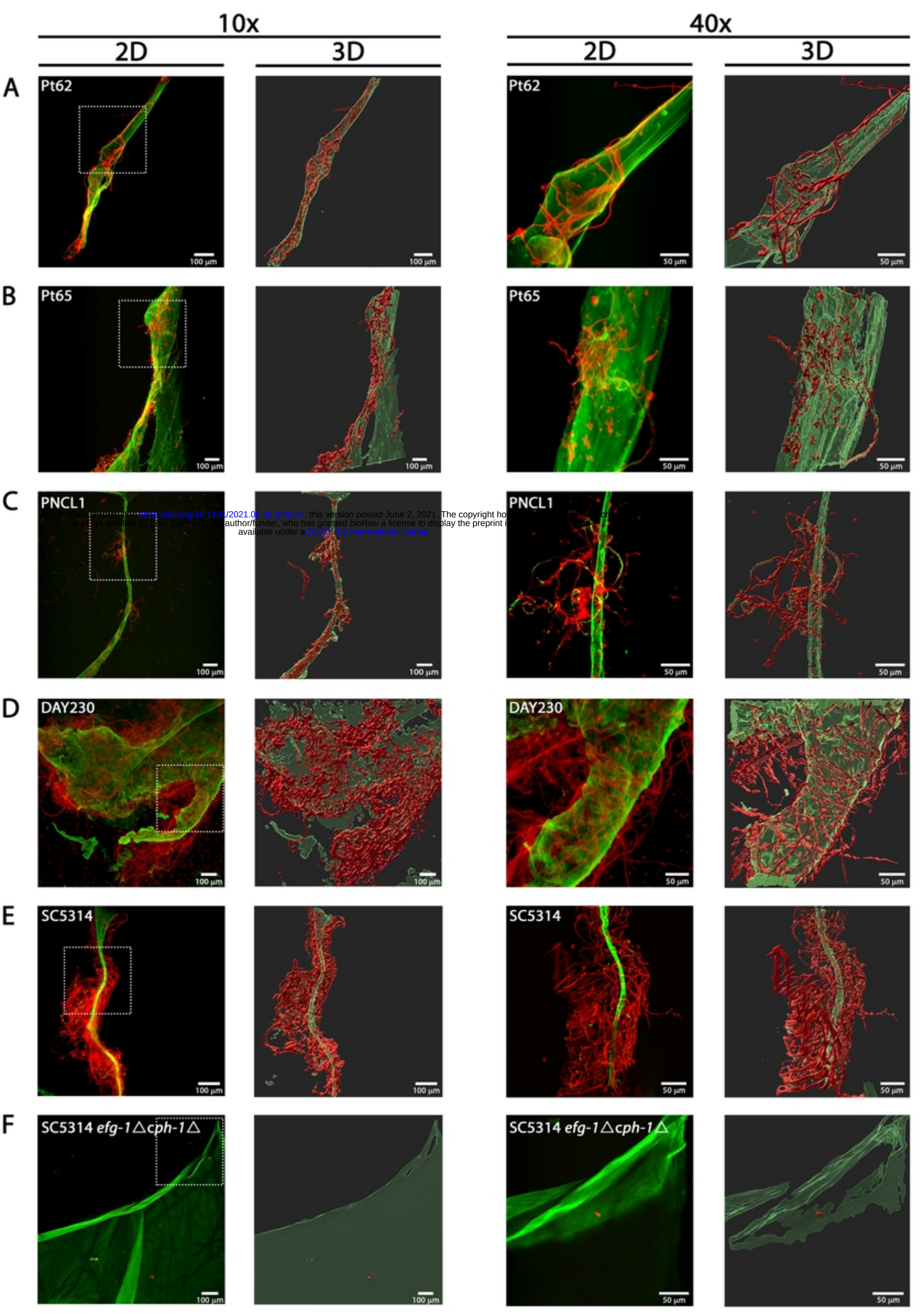

Figure 4

bioRxiv preprint doi: https://doi.org/10.1101/2021.06.01.446547; this version posted June 2, 2021. The copyright holder for this preprint (which was not certified by peer review) is the author/funder, who has granted bioRxiv a license to display the preprint in perpetuity. It is made available under aCC-BY 4.0 International license.

A

Pt62

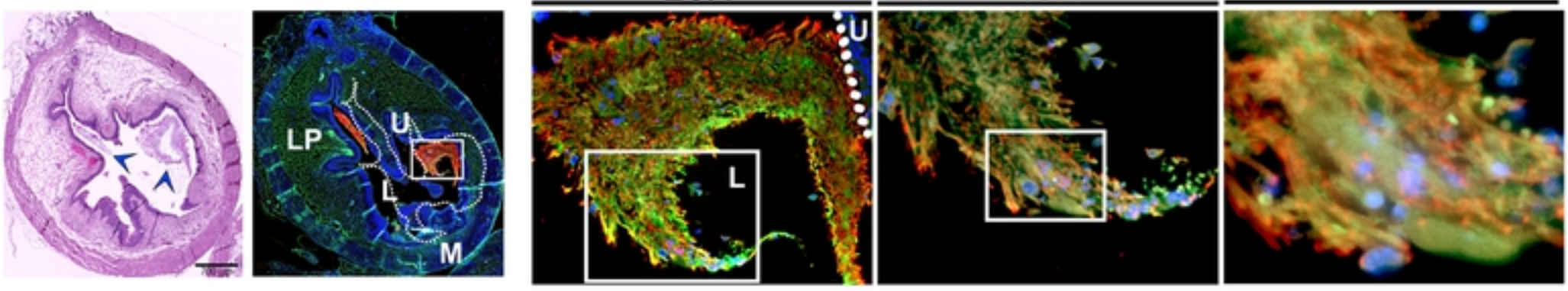

B

Pt65

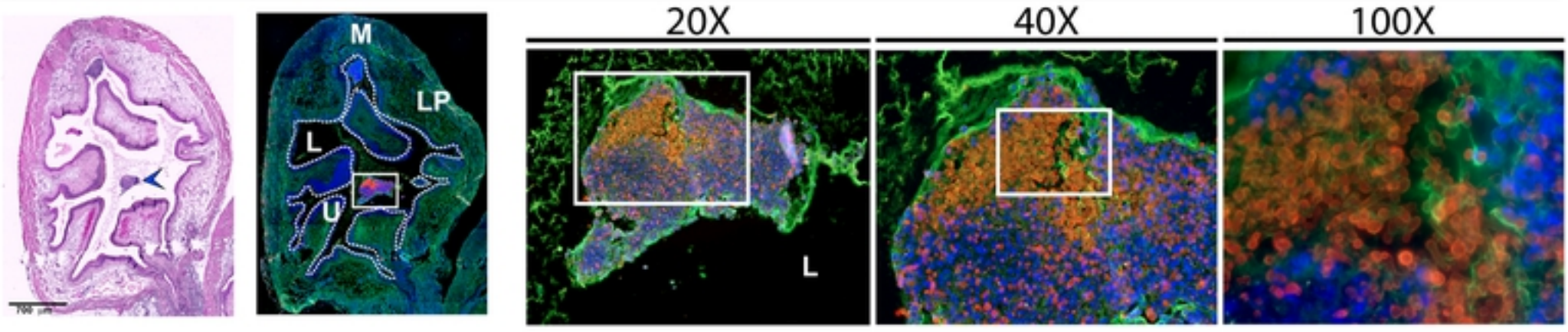

C

PNCL1

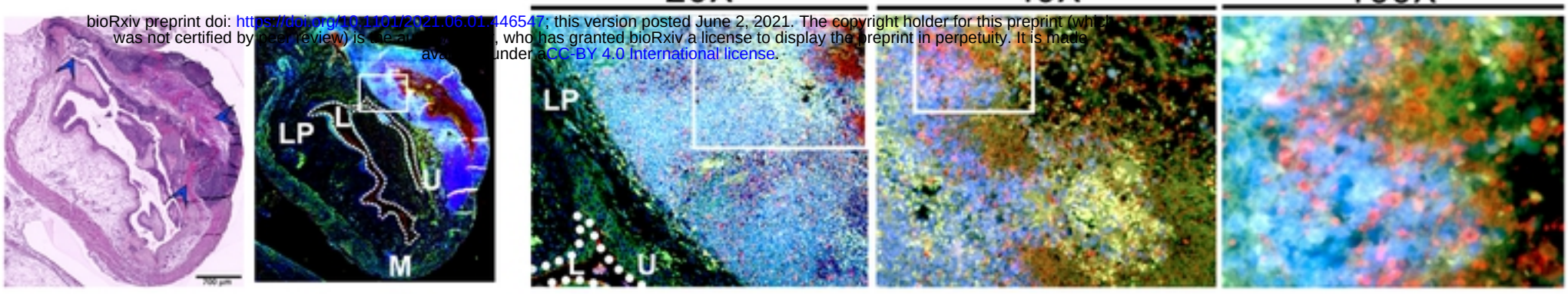

D

DAY230

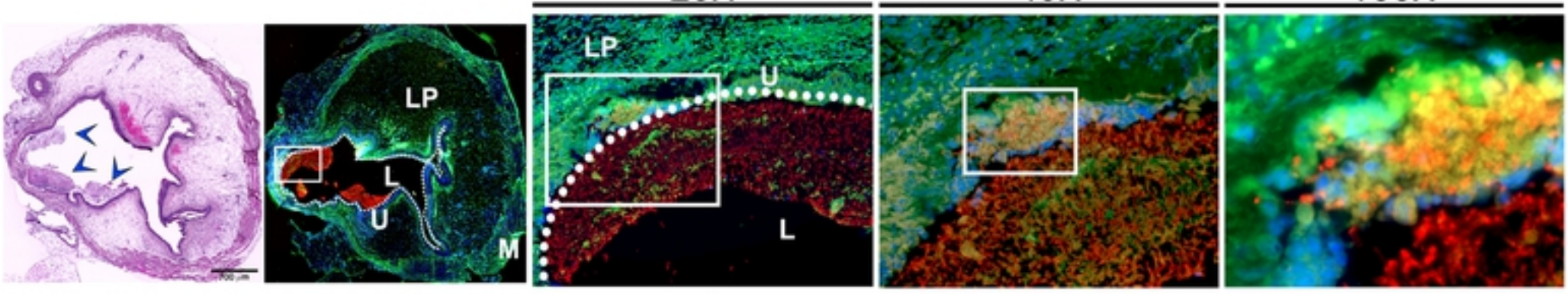

E

SC5314

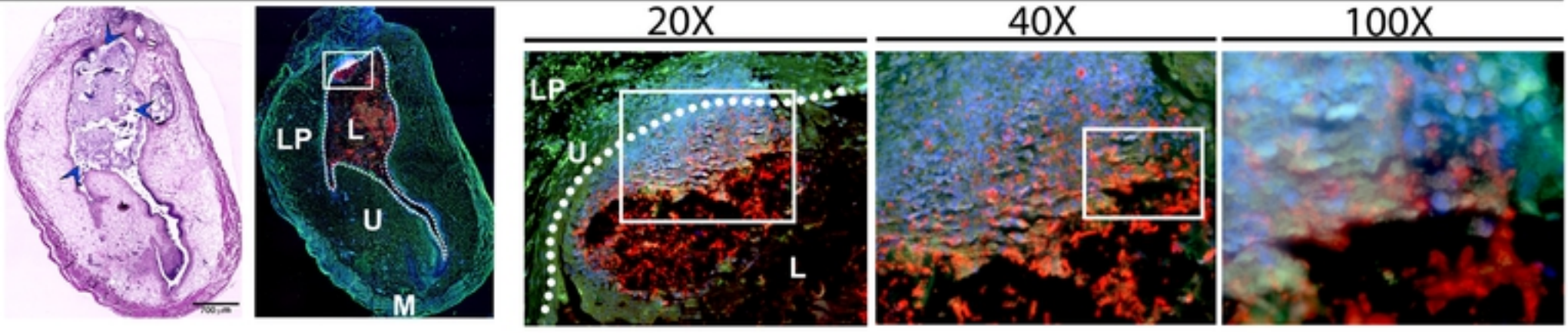

F

SC5314 *efg-1△cph-1△*

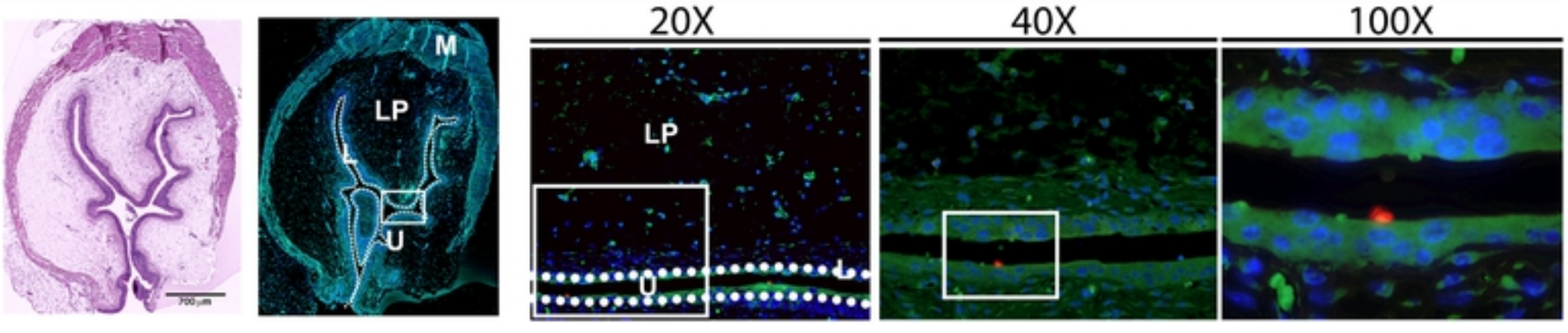

Figure 6

bioRxiv preprint https://doi.org/10.1101/2021.06.01.446547 ... CC-BY 4.0 International license

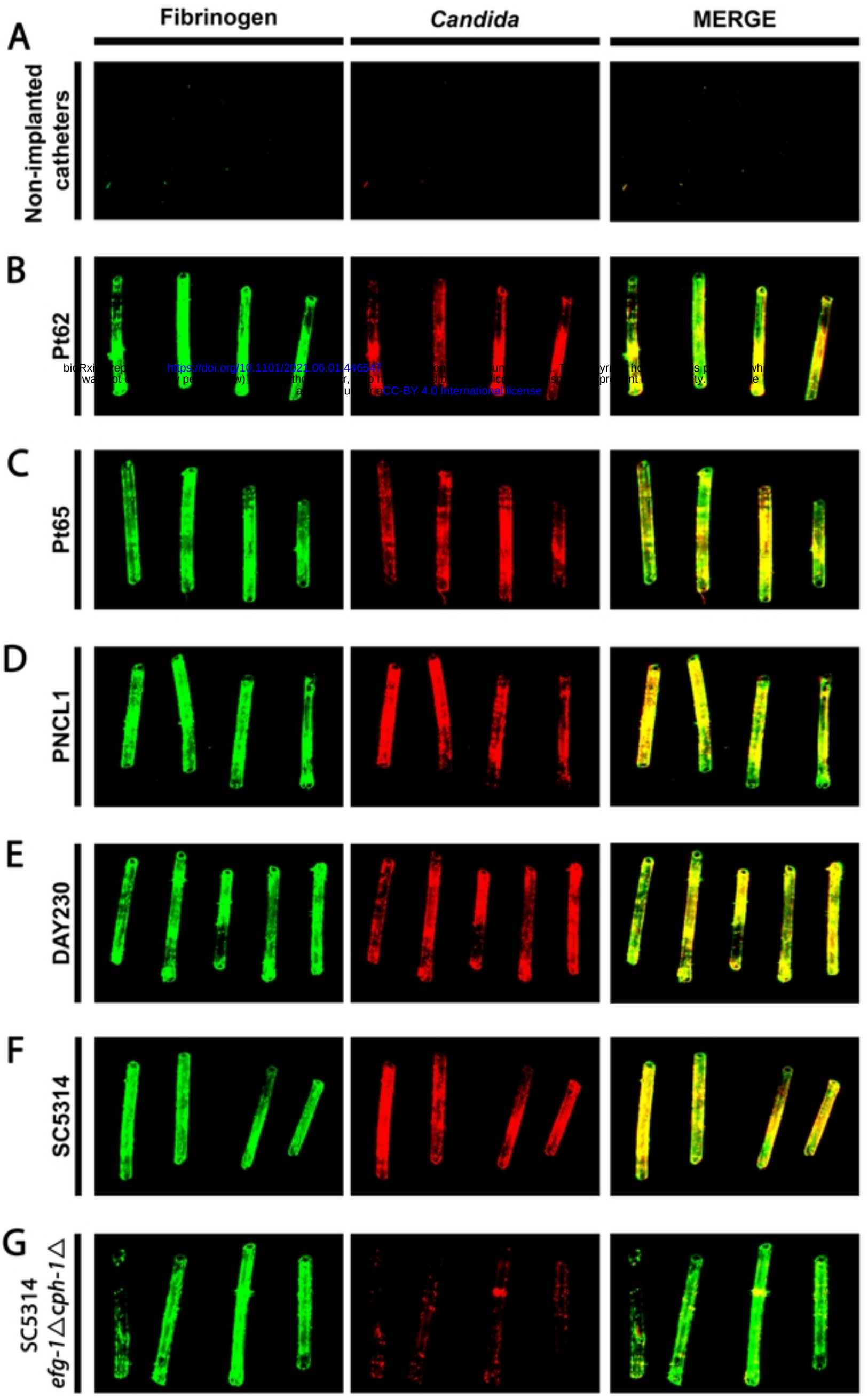

Figure 7

bioRxiv preprint doi: https://doi.org/10.1101/2021.06.01.446547; this version posted June 2, 2021. The copyright holder for this preprint (which was not certified by peer review) is the author/funder, who has granted bioRxiv a license to display the preprint in perpetuity. It is made available under aCC-BY 4.0 International license.

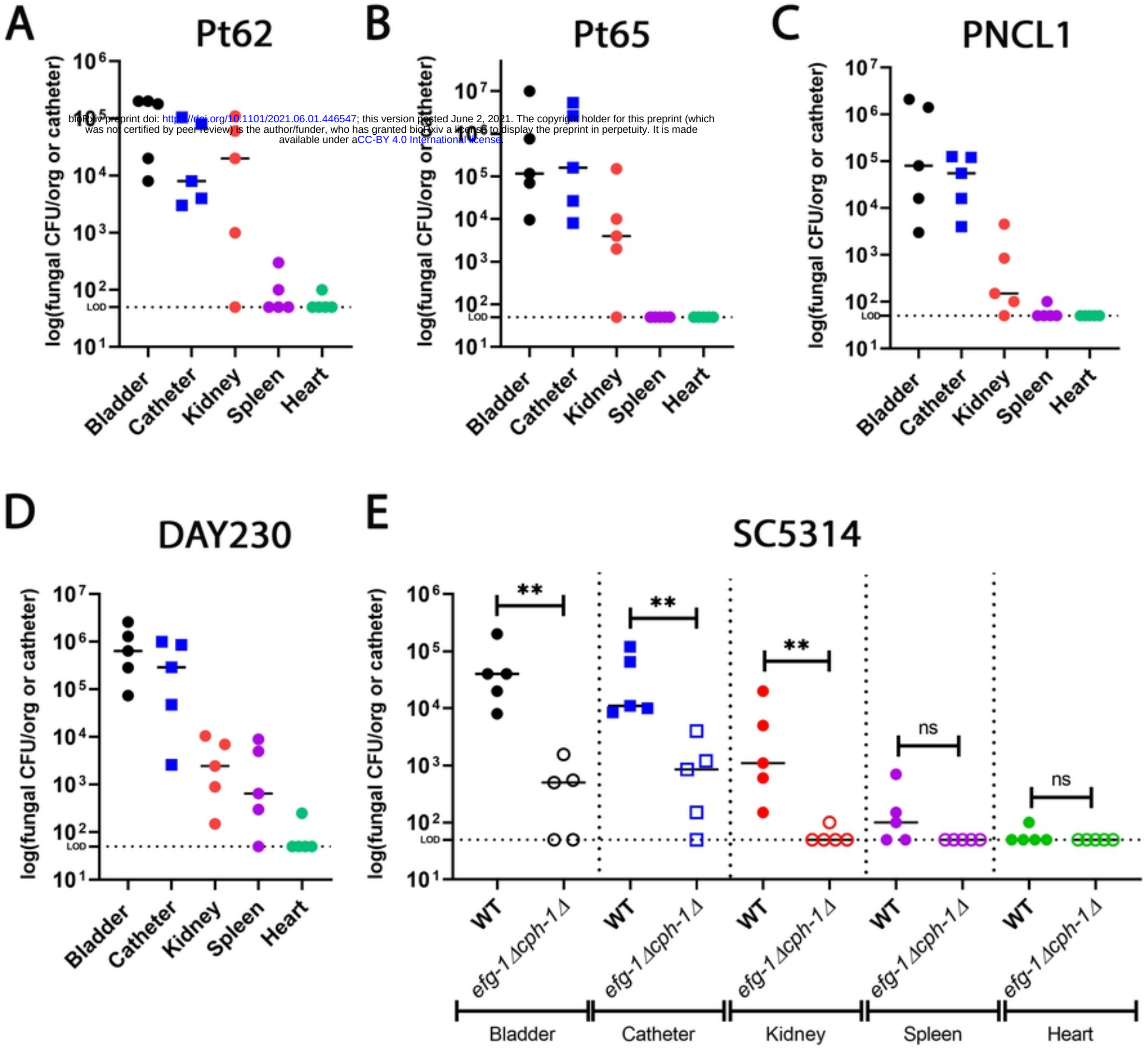

Figure 5